Outline #4 Dating Geologic Materials and Landforms

Timescales of climatic variation
-short-term (high frequency) vs long-term (low frequency variation

Dating Glacial Deposits and Landforms
-Relative vs Absolute (Numerical) Dating
-Bracketing Ages (maximum vs minimum ages)

Relative Dating Techniques
-stratigraphic relationships
-landform morphology change
-weathering parameters
-soil chronosequences

Numerical Dating Techniques
-radiocarbon dating
-potassium argon dating
-fission track dating
-uranium-series dating
-thermoluminescence dating
-cosmogenic isotope dating

Age-Equivalent Stratigraphic Markers
-paleomagnetism
-tephrochronology

Incremental Dating Techniques
-dendrochronology
-varve chronology
-lichenometry

Numerical Dating Methods

Numerical ages can be assigned to geologic materials using 1. radiometric dating, where radioactive parent atoms decay to radiogenic daughter atoms, 2. using age-equivalent stratigraphic markers, which require independent dating of the stratigraphic marker and 3. incremental methods, which rely upon annual biogenic growth patterns or annual sediment accumulation.

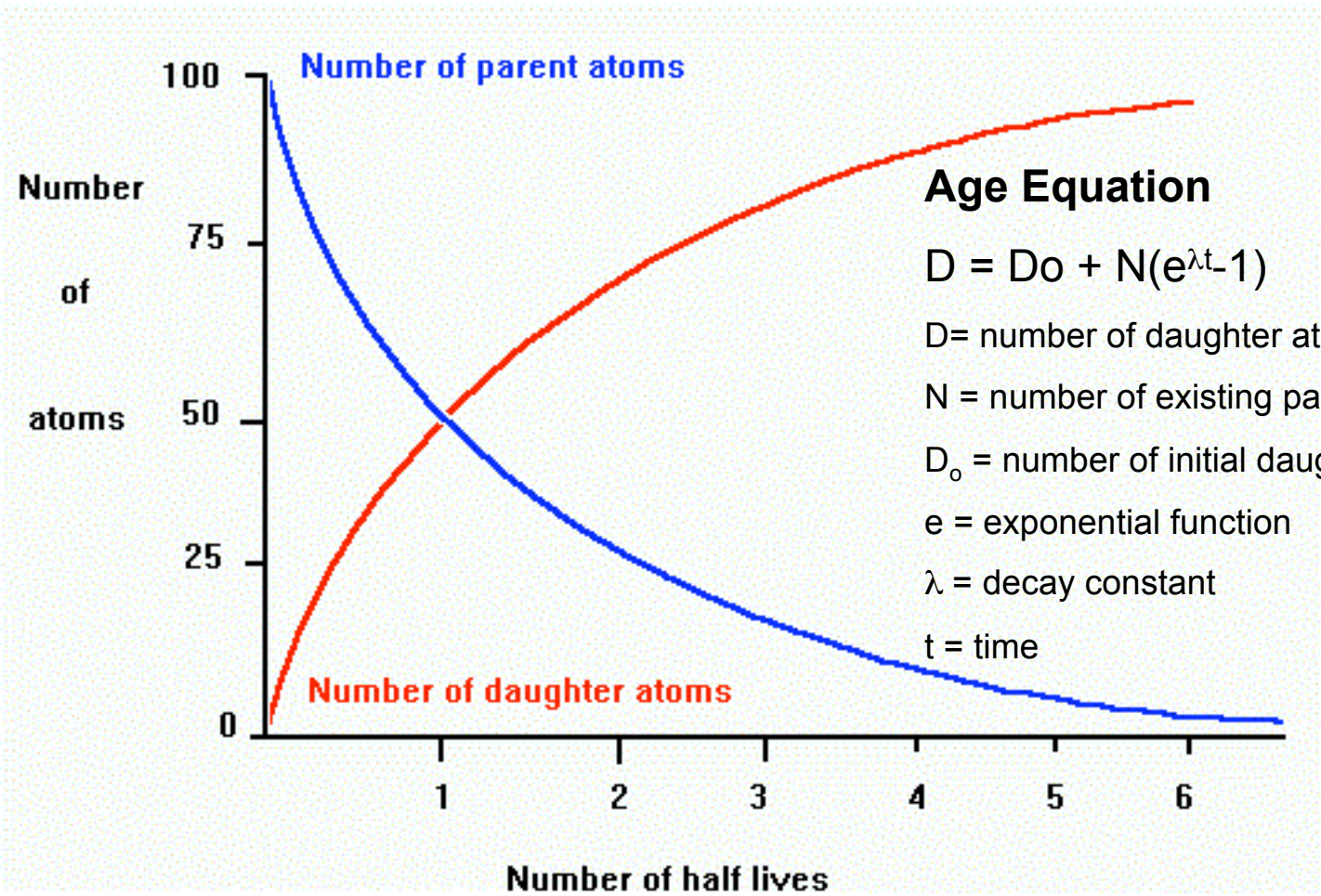

Radioactive isotopes will decay spontaneously to form daughter atoms. Radioactive decay is exponential and constant. Different radioactive elements will have different decay rates, but the decay curve will be the same (shown as blue curve). As radioactive parent atoms decay, daughter atoms are correspondingly created (shown as red curve). If you can measure the ratio of parent to daughter atoms in a isotope system, you can solve for the age (t). **$T = 1/\lambda \ln[(D - D_0)/N + 1.$**

Radioactive Decay Processes

Simple Decay: represents a decay process where a radioactive isotope will decay to a single radiogenic daughter atom. For example, radiocarbon (^{14}C) will always decay to nitrogen (^{14}N).

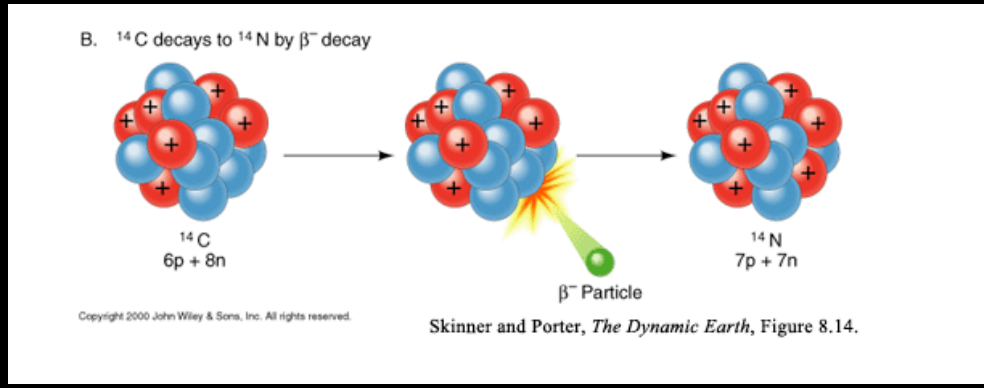

Branched Decay: represents a decay process where the radioactive isotope can decay to more than one radiogenic daughter atom. For example ^{40}K can decay to either ^{40}Ca (88.2% of the time) or ^{40}Ar (11.8% of the time).

$$^{40}_{19}K \rightarrow {}^{40}_{20}Ca + {}^{0}_{-1}e + {}^{0}_{0}\bar{\nu} \quad \text{(beta decay)}$$

$$^{40}_{19}K \rightarrow {}^{40}_{18}Ar + {}^{0}_{+1}e + {}^{0}_{0}\nu \quad \text{(positron emission)}$$

$$^{40}_{19}K + {}^{0}_{-1}e \rightarrow {}^{40}_{18}Ar + {}^{0}_{0}\nu \quad \text{(electron capture)}$$

Radioactive Decay Processes

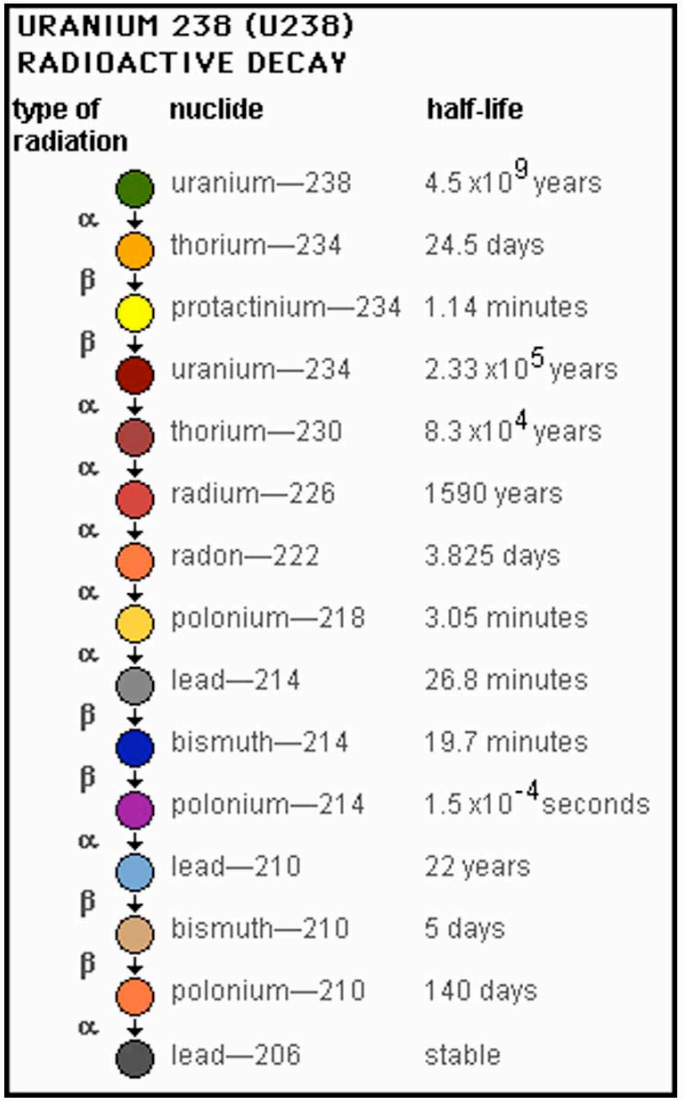

A chain decay involves the radioactive decay of intermediate radioactive daughter atoms that eventually decay to stable daughter such as the decay of ^{238}U to ^{206}Pb.

Isotope		Half-life of parent (years)	Useful range (years)
Parent	Daughter		
Carbon 14	Nitrogen 14	5,730	100 - 30,000
Potassium 40	Argon 40	1.3 billion	100,000 - 4.5 billion
Rubidium 87	Strontium 87	47 billion	10 million - 4.5 billion
Uranium 238 Uranium 235	Lead 206 Lead 207	4.5 billion 710 million	10 million - 4.6 billion

The decay constant and half-life (The half life is the time it takes one half of the existing parent atoms to decay to daughter atoms) of a radionuclide are related mathematically:

$$T_{1/2} = 0.693/\lambda$$

Generally, the greater the half-life of a radioactive isotope pair the greater the age range for dating purposes.

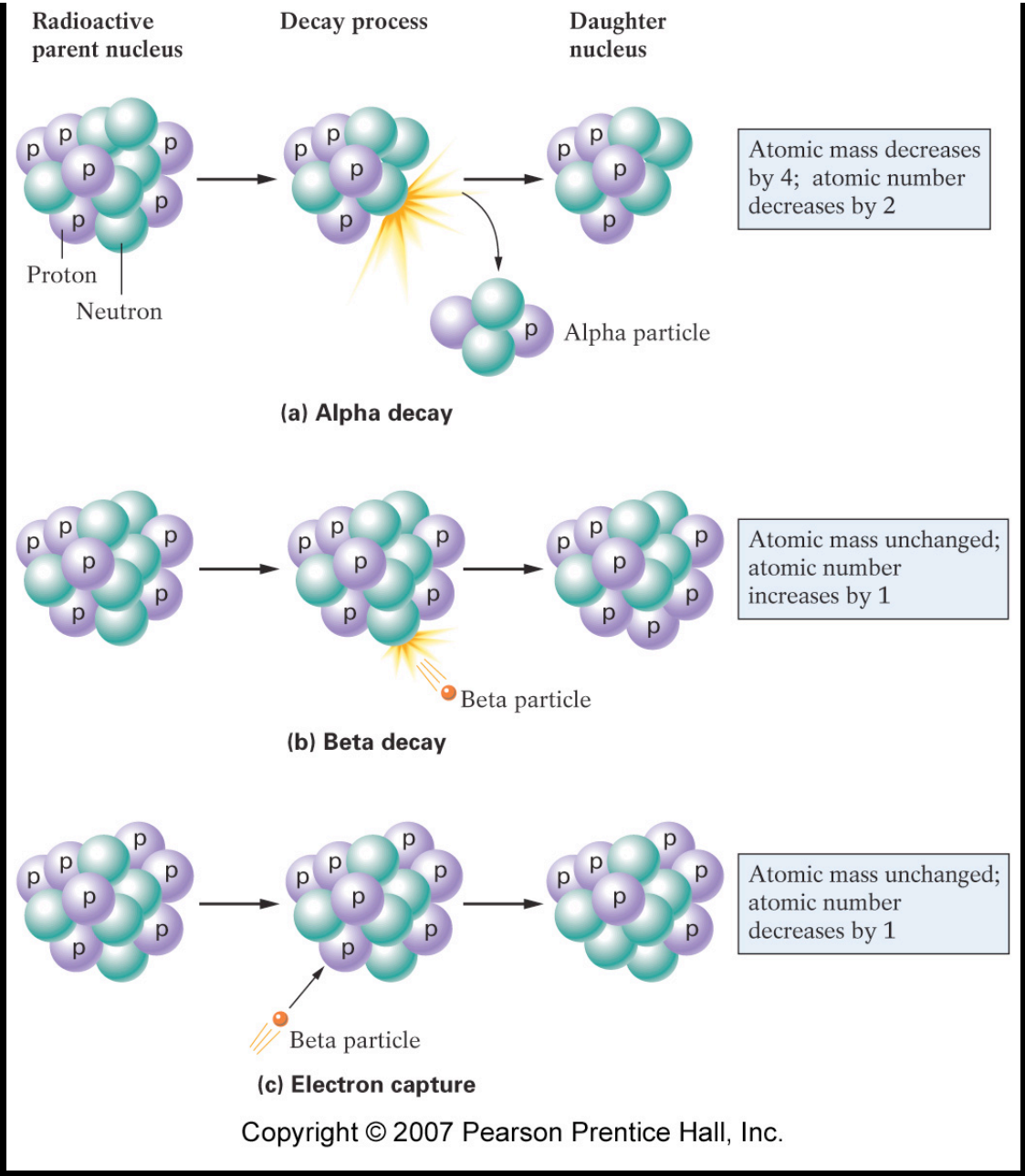

Radioactive decay occurs via three decay processes: Alpha Decay, Beta Emission, Electron Capture.

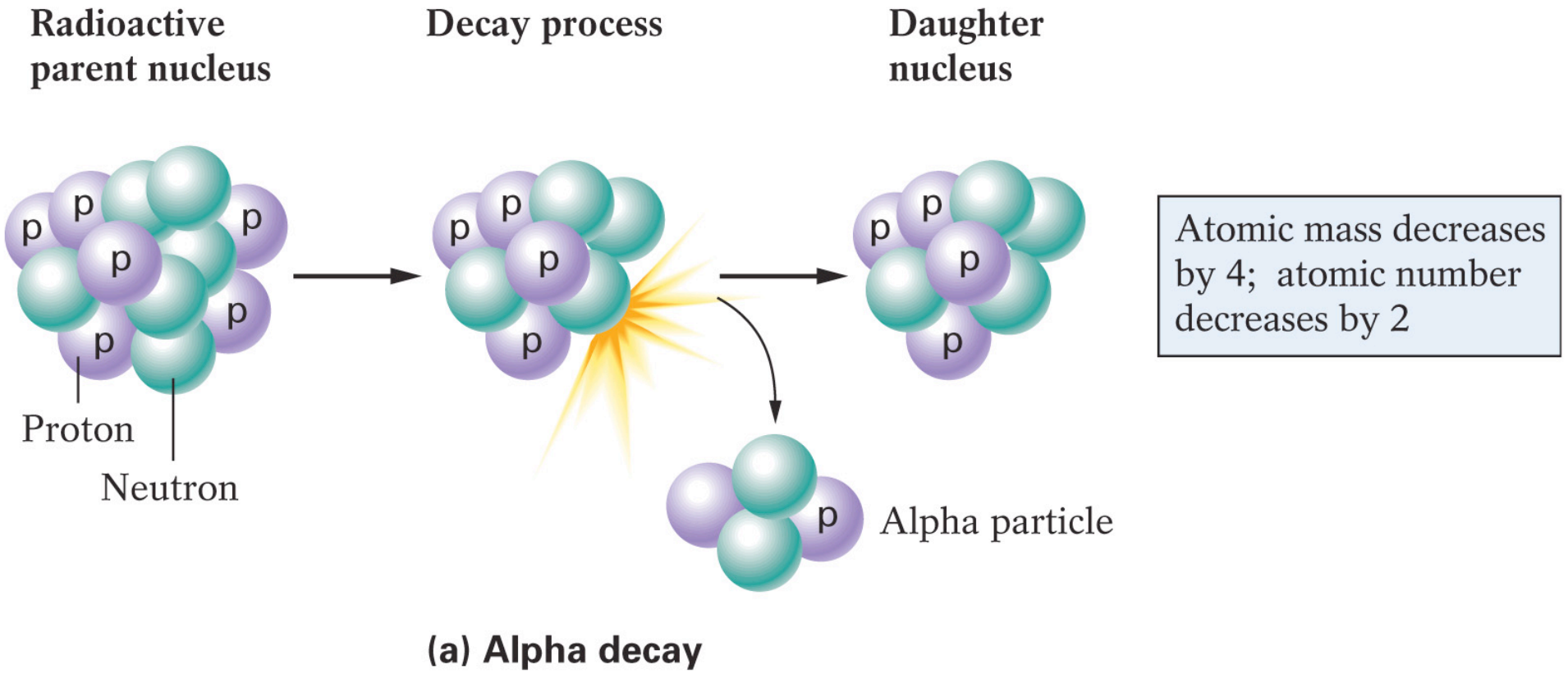

(a) Alpha decay

Alpha decay: the nucleus of the radioactive isotope emits and alpha (α) particle, comprising of 2 neutrons and 2 protons. The atomic number of the isotope decreases by 2, while the mass number decreases by 4. ^{234}U decays to ^{230}Th by alpha decay.

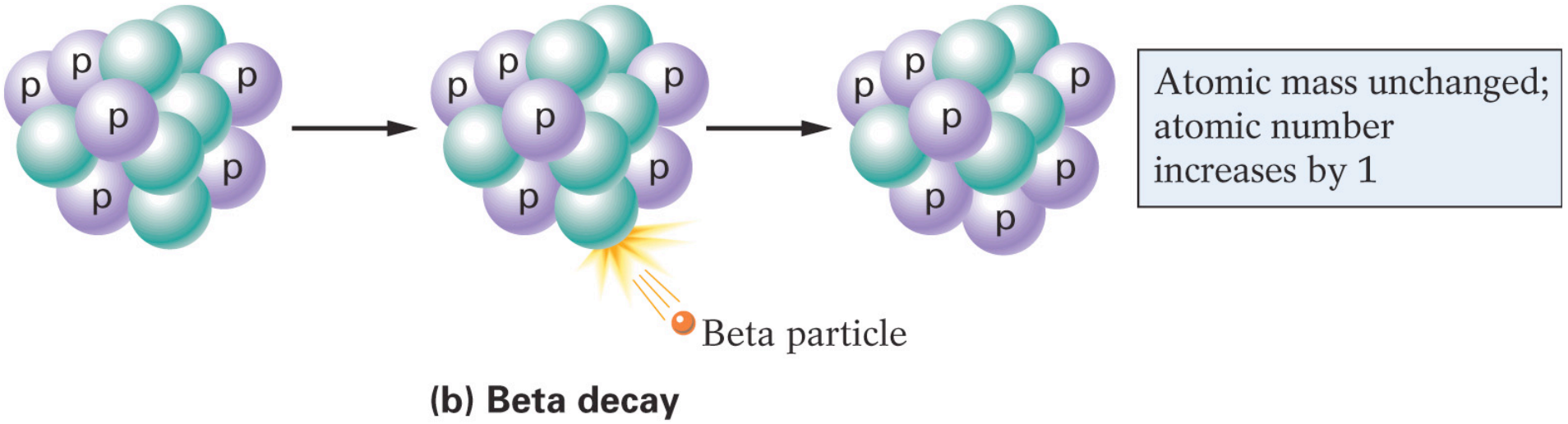

(b) Beta decay

Beta Emission (Decay): a neutron emits a beta (β) particle (similar to an electron) and is tranformed into a proton. The atomic number of the atom has increased by one while the mass number remains unchanged. The decay of ^{14}C to ^{14}N occurs via $\beta-$ emission.

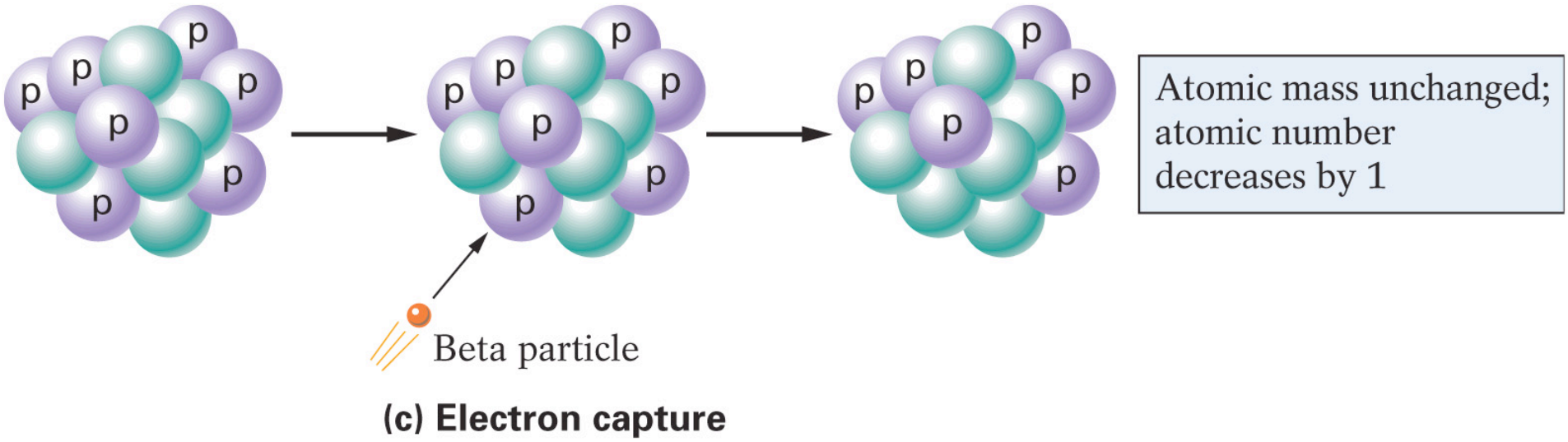

(c) Electron capture

Electron (β)- Capture: a proton captures an electron and is transformed into neuton and emits a gamma (γ) particle. The atomic number of the atom has decreased by one while the mass number remains unchanged. The decay of ^{40}K to ^{40}Ar occurs via β–capture.

Potassium-Argon Dating

^{40}K decays to ^{40}Ar (11.8% probability) and ^{40}Ca (88.2% probability) via a branched decay.

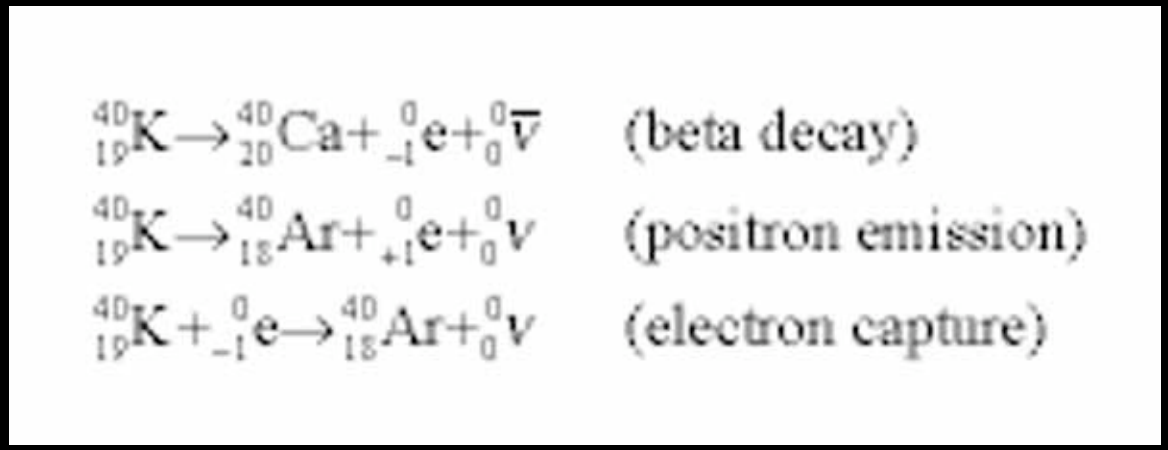

Only ^{40}K - ^{40}Ar decay is useful for dating earth rocks because ^{40}Ca is ubiquitous in rock (i.e., plagioclase) and cannot be differentiated from the radiogenic ^{40}Ca produced from decay of ^{40}K. Ages can be calculated by measure the parent and daughter ratios and compensating for the branched decay.

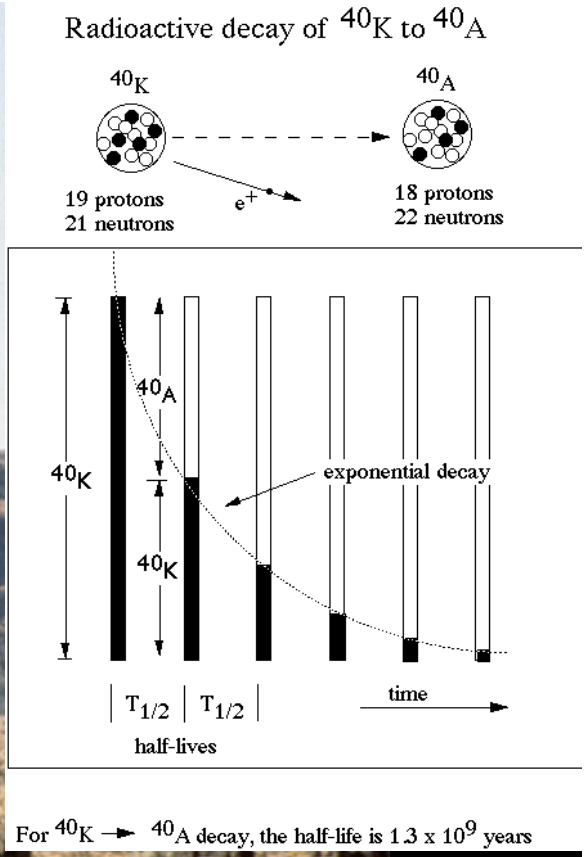

For $^{40}K \rightarrow {}^{40}A$ decay, the half-life is 1.3×10^9 years

Potassium-Argon has a half-life of 1.3 billion years and is useful for dating K-rich minerals that have and age range between 100,000 years and 4.6 billion years. Rocks with lower potassium content, such as basalt, will have greater uncertainty at the younger end of the age range.

The steep front of this Hawaiian basalt flow represents an ice-contact front. The basalt flow abutted against glacial ice and its K-Ar age provides constraints on the timing of glacial advance on the Big Island of Hawaii.

The range front fault (trace shown by dotted line) exposed along the eastern Sierra Nevada cross-cuts a basaltic cinder cone that was dated using K-Ar dating. How could this age be used to constrain the uplift rate along this fault and the timing of uplift of the Sierra Nevada ?

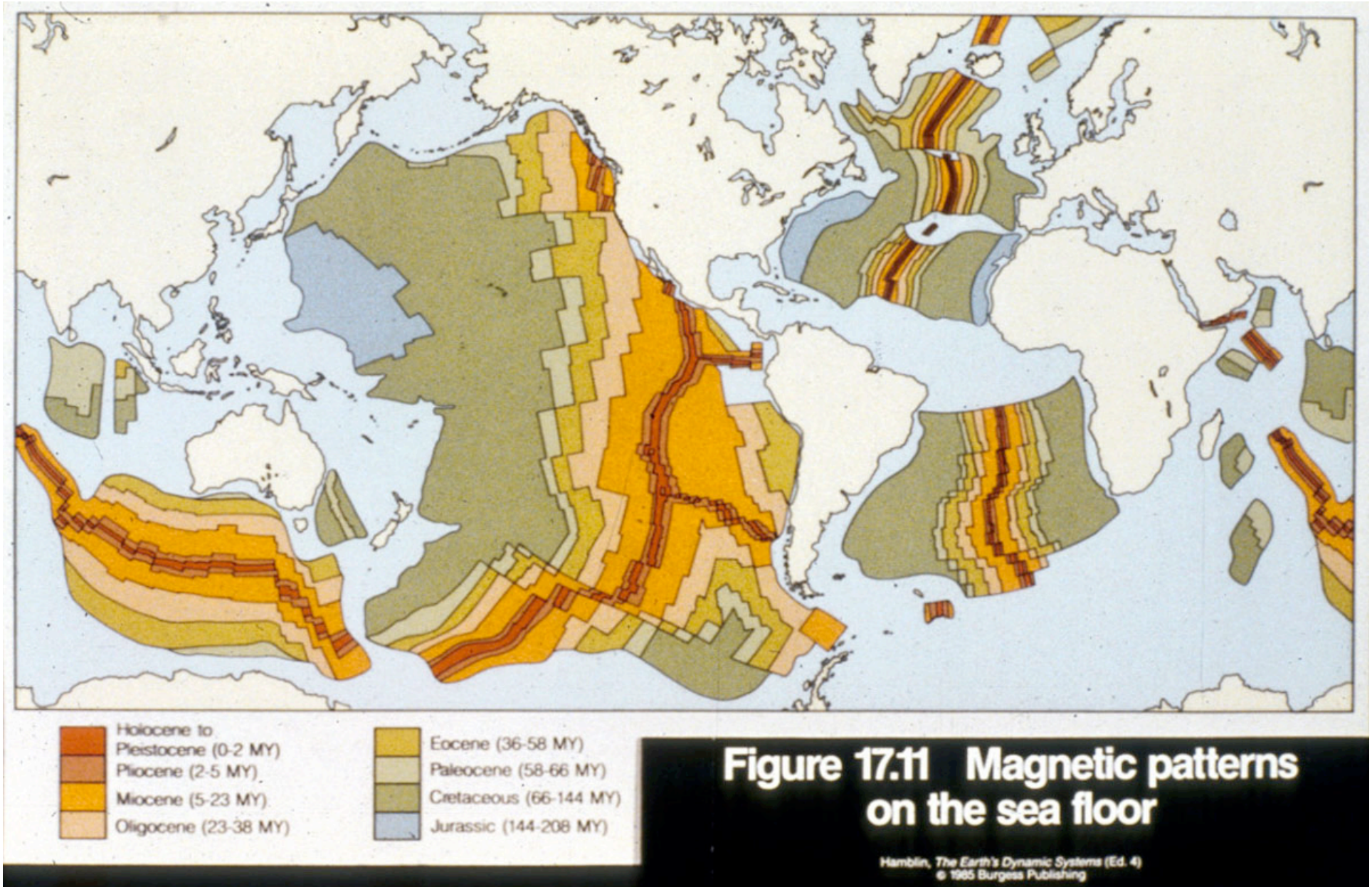

Figure 17.11 Magnetic patterns on the sea floor

Hamblin, *The Earth's Dynamic Systems* (Ed. 4)

K-Ar dating has been used to date the basaltic ocean lithosphere and assign ages to polarity changes preserved in the ocean floor.

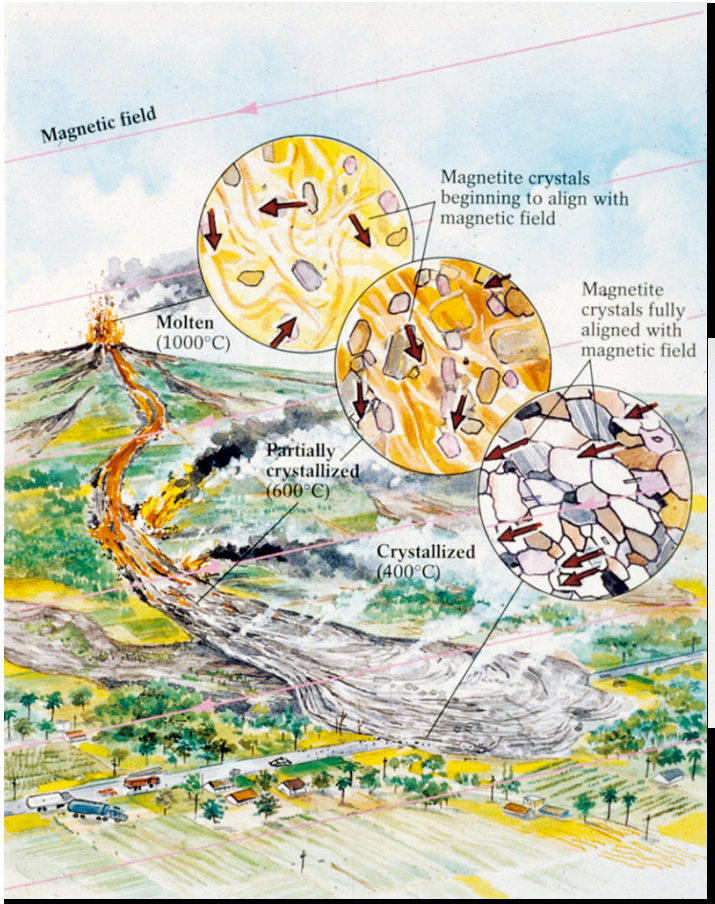

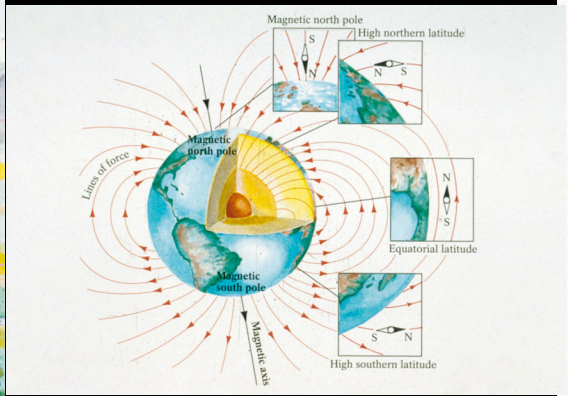

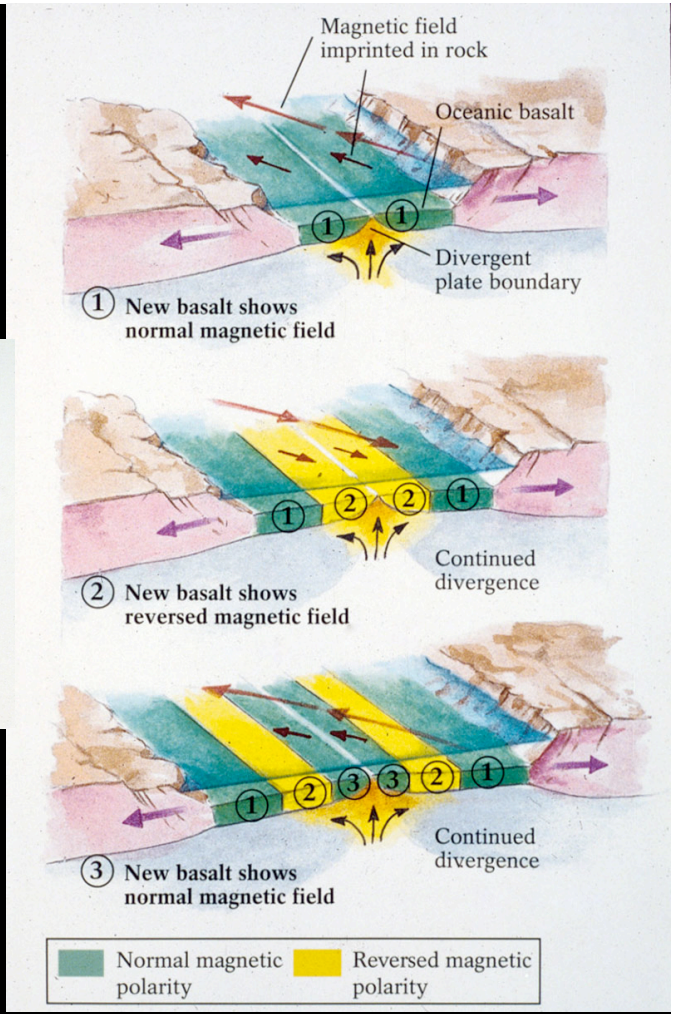

The earth's magnetic signature (polarity changes and inclination of the prevailing magnetic field) is preserved in mafic rock. As the magma or lava crystallizes, the magnetic minerals will be aligned with the prevailing magnetic field and be preserved in the rock.

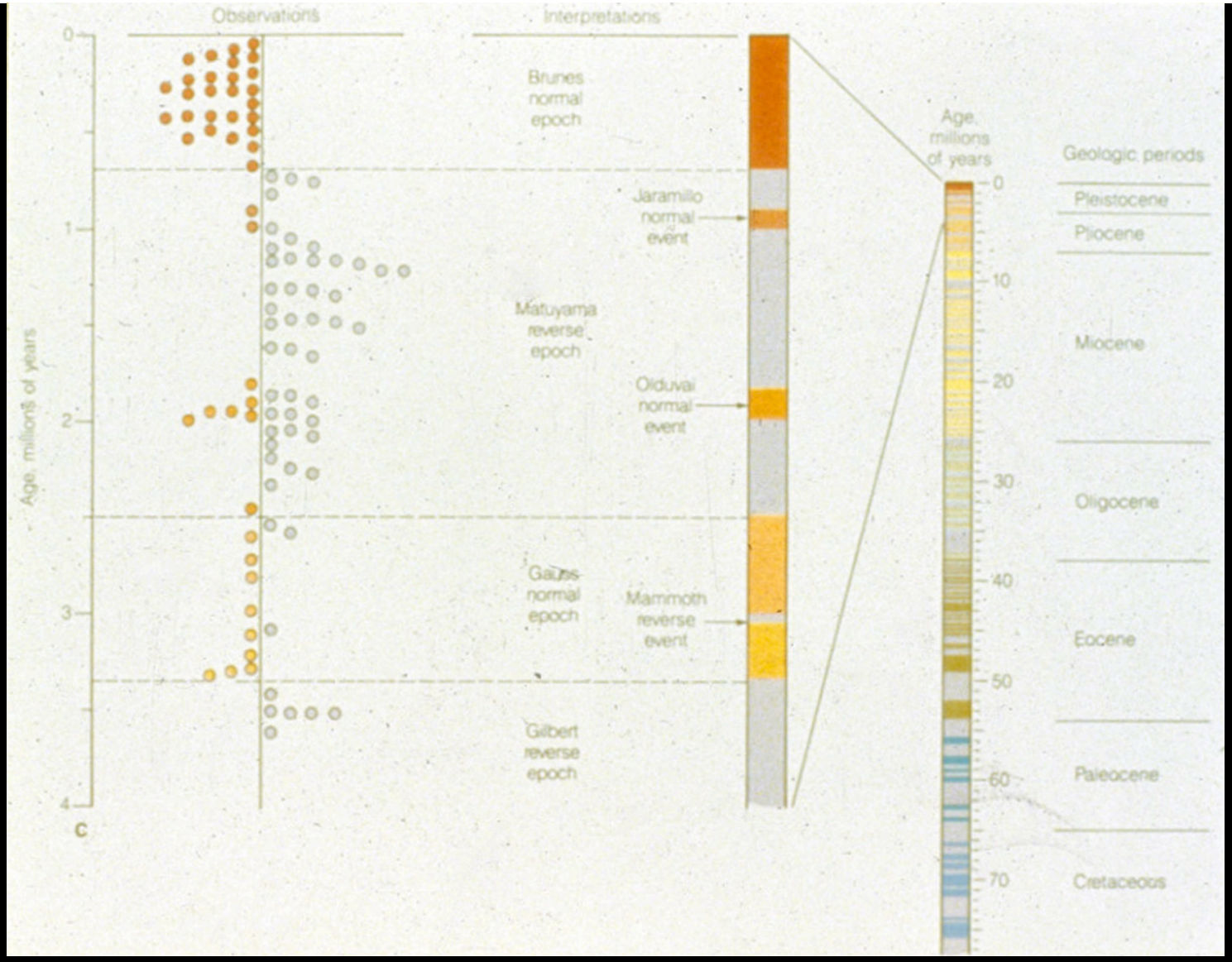

K-Ar dating has been very important in assigning ages to the timing of polarity changes and establishing the paleomagnetic time scale (portion shown above).

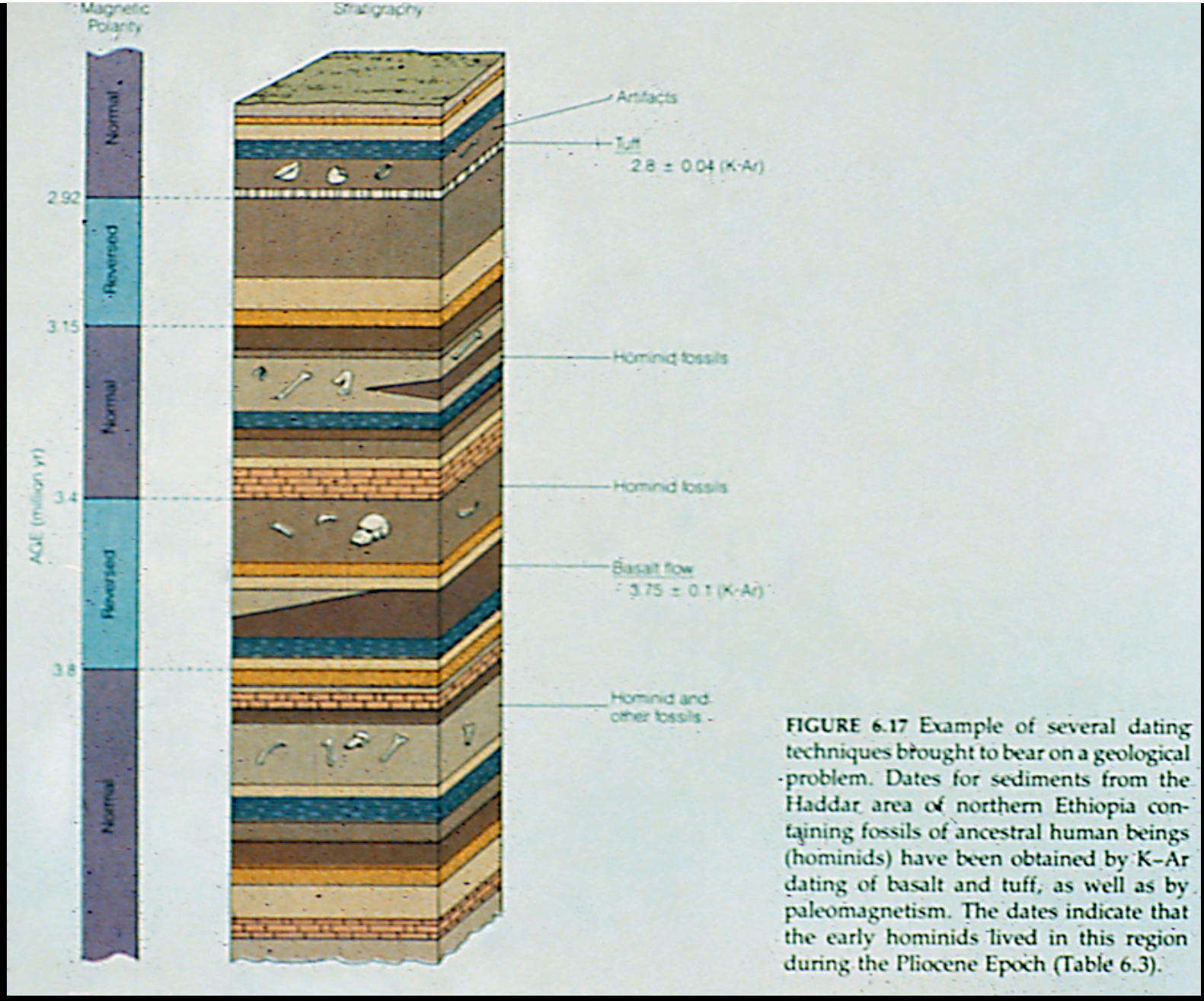

FIGURE 6.17 Example of several dating techniques brought to bear on a geological problem. Dates for sediments from the Haddar area of northern Ethiopia containing fossils of ancestral human beings (hominids) have been obtained by K–Ar dating of basalt and tuff, as well as by paleomagnetism. The dates indicate that the early hominids lived in this region during the Pliocene Epoch (Table 6.3).

K-Ar dating was utilized to assign chronology of early hominid finds in northern Ethiopia. Paleomagnetic ages can be used to fill in gaps within the chronology.

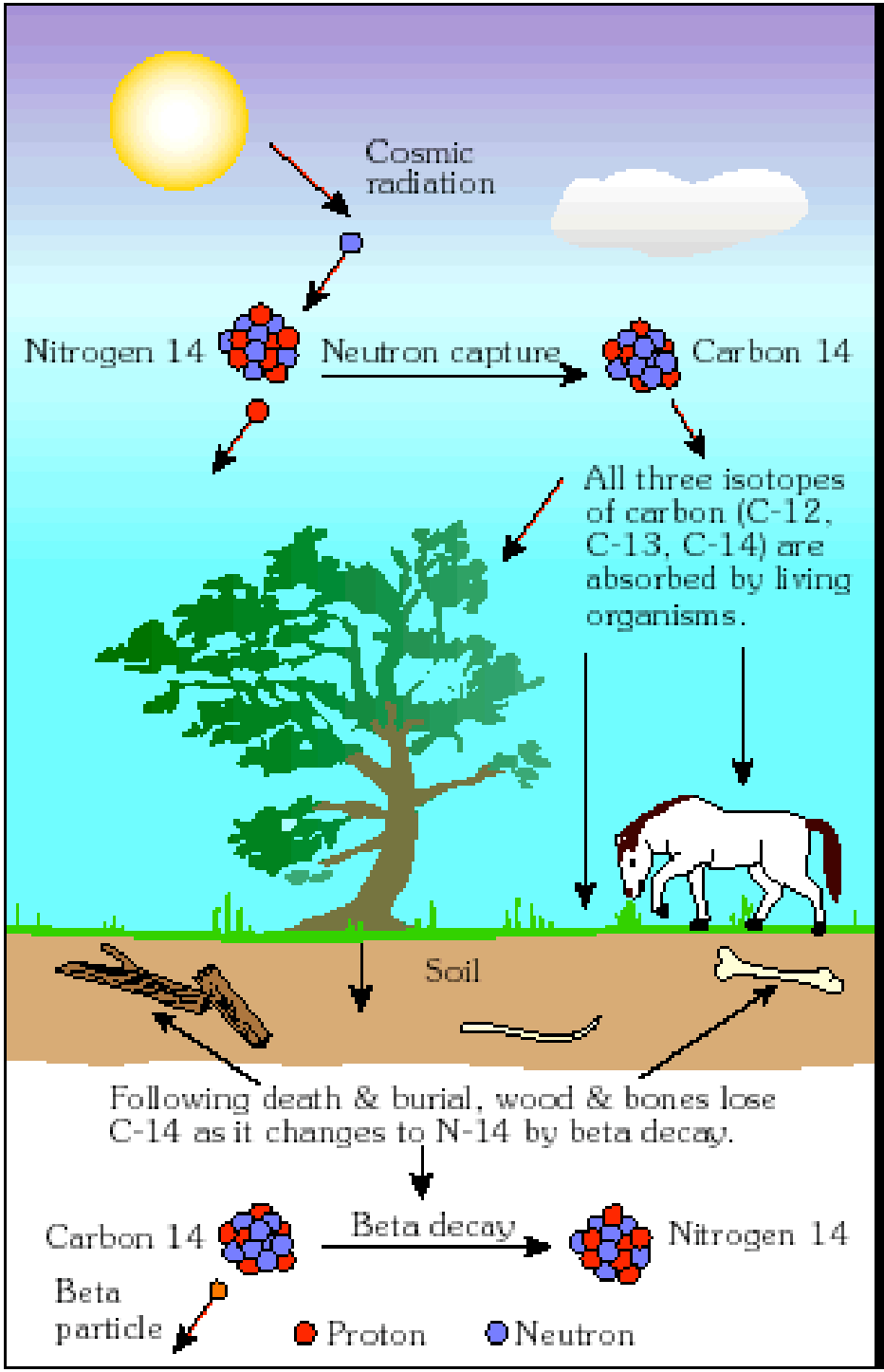

Radiocarbon is first produced in the atmosphere by collisions of neutrons with nitrogen atoms (Nitrogen has 7 protons and 7 neutrons in its nucleus).

The neutron will knock out a proton from the nitrogen atom's nucleus, replacing it with a neutron. The proton number is reduced by 1 (it is now 6), but the mass number remains the same (14).

The atom will now have 6 protons and 8 neutrons in its nucleus and form the isotope ^{14}C (radiocarbon). C-14 is radioactive and decays with a half-life of 5730 years back to Nitrogen (^{14}N).

The ^{14}C atoms rapidly form CO_2 gas and then exchanged between the atmosphere, hydrosphere and biosphere. As long as the organism is alive it will continually exchange carbon within its reservoir and remain in equilibrium as new carbon is replenished. After the organism dies the ^{14}C clock is set as the ratio of ^{14}C/stable carbon (^{12}C and ^{13}C) decreases as ^{14}C decays to ^{14}N.

Radiocarbon Decay Activity

^{14}C decays to ^{14}N as it emits a beta (β) particle. "Modern" carbon has an a decay activity of ~15 dpm/gm. The decay activity (Beta emission rate) will decrease by 50% every half-life (5730 years). Radiocarbon ages can be determined for organic matter by counting β-emissions.

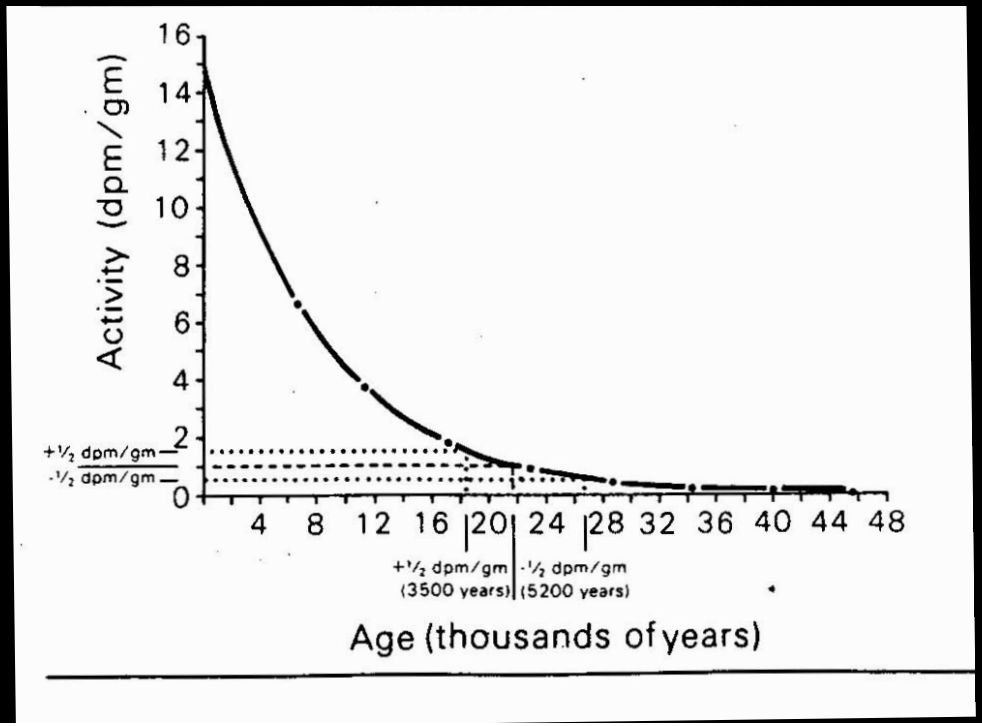

Isotopic Fractionation

There are three naturally occurring isotopes of carbon:

98.9% 12C, 1.1%13C, both stable and 1.18 X 10^{-10}% ^{14}C, radioactive.

In nature fractionation of this ratio occurs, where photosynthesis results in the enrichment of ^{12}C relative to the heavier isotopes, where as ocean water preferentially absorbs ^{14}C relative to the lighter isotopes.

In nature it has been found that $^{14}C/^{12}C$ is double the fractionation of $^{13}C/^{12}C$.

$$\delta^{13}C = (^{13}C/^{12}C_{sample} - {}^{13}C/^{12}C_{standard}) / {}^{13}C/^{12}C_{standard} \times 1000$$

*Standard is PDB limestone (belemite carbonate from the Cretaceous Peedee Formation, South Carolina

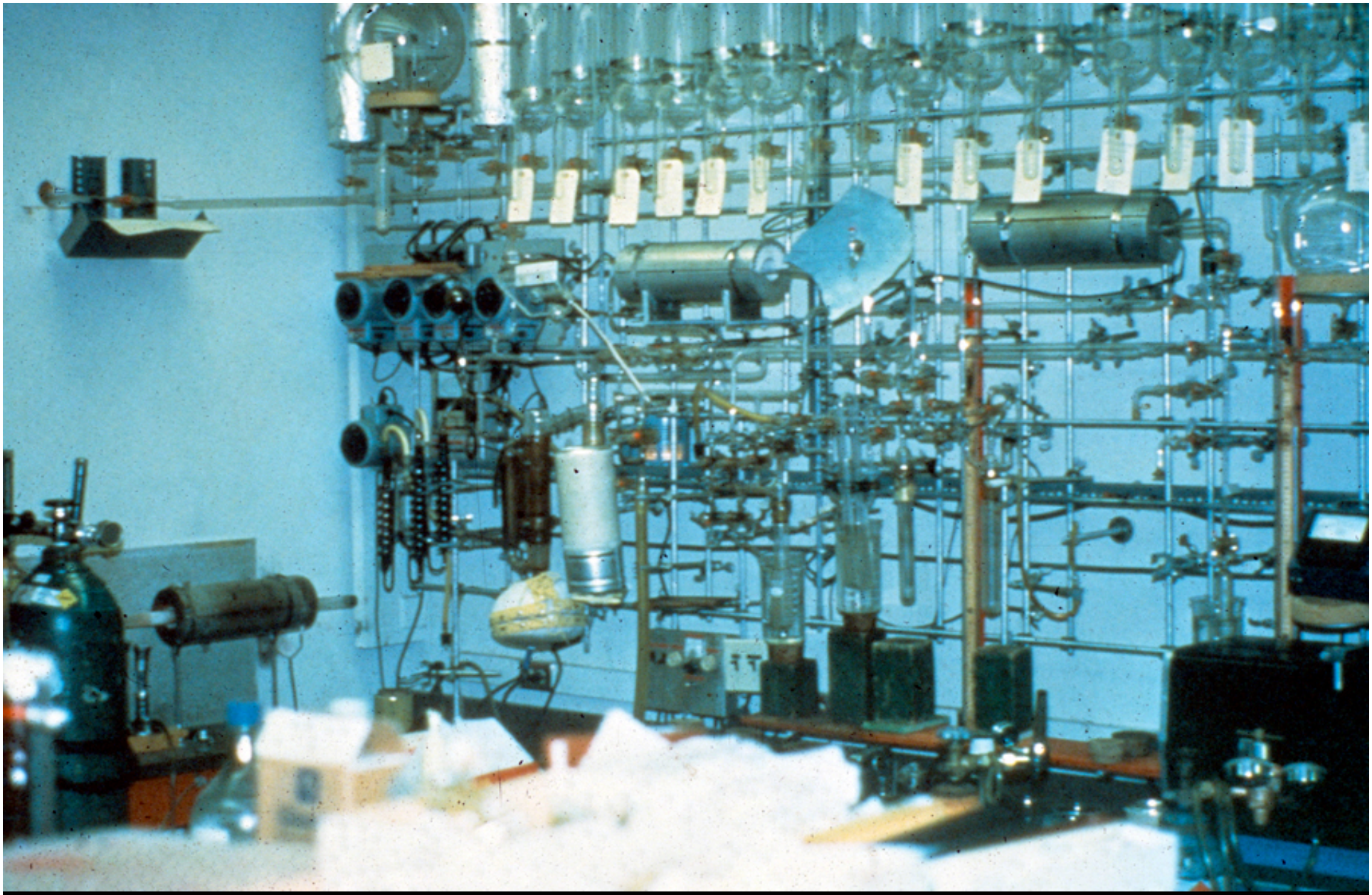

Organic samples are prepared for radiocarbon dating by combusting or dissolving the organics and producing CO_2 gas. The decay activity in the CO_2 gas will be directly related to the time of death (age) of the organic material.

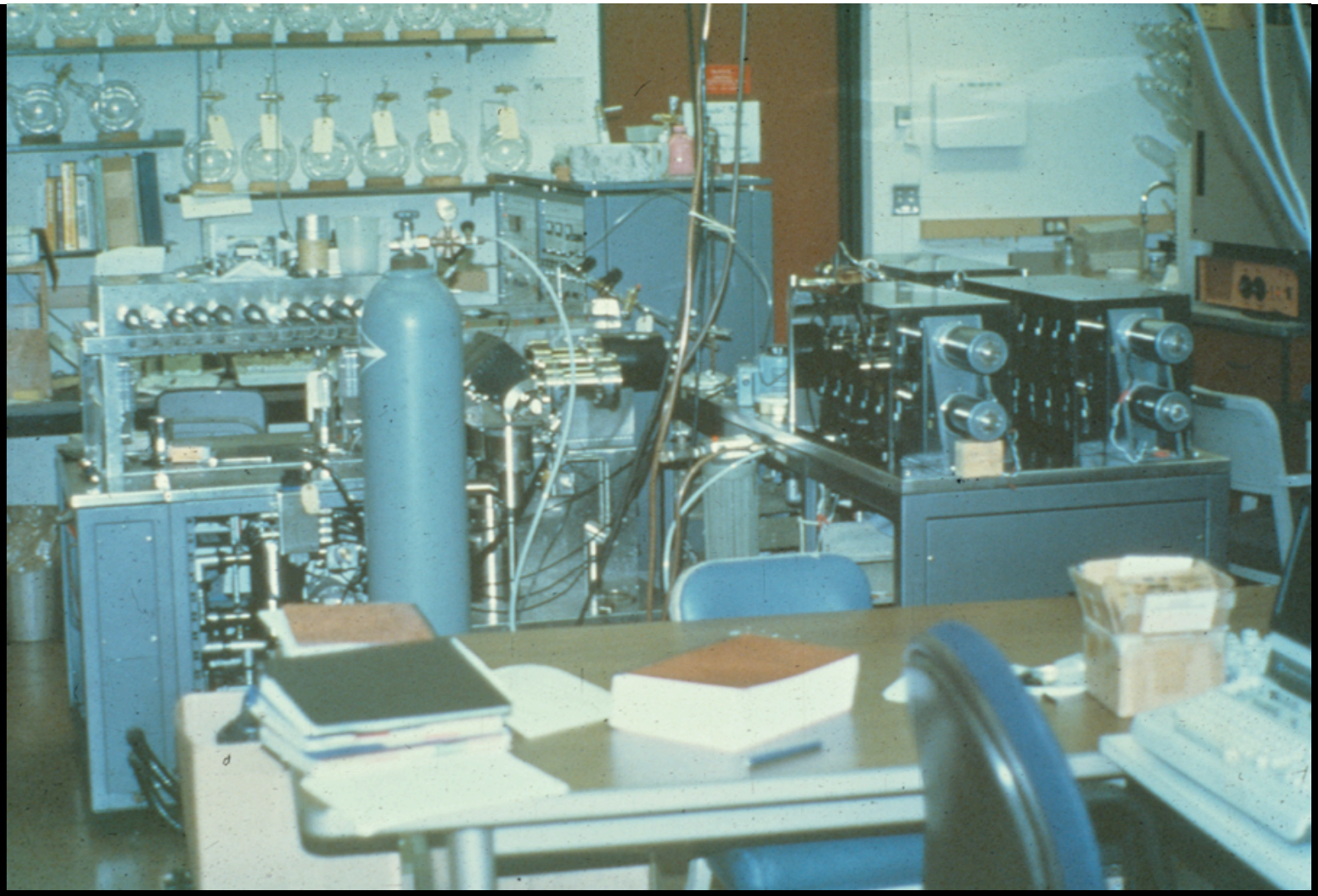

Beta-counting laboratories, such as the one shown above, determine ^{14}C ages based on the measured ^{14}C activity (decay counting) of the organic sample. A liter of CO_2 gas combusted from a modern piece of wood (i.e., assigned to 1950 AD and compensating for bomb and industrial revolution effects) would have a b-decay count of 15 decays per minute. What would the decay rate be for a piece of wood that was 5730 (1 half-life) years old?

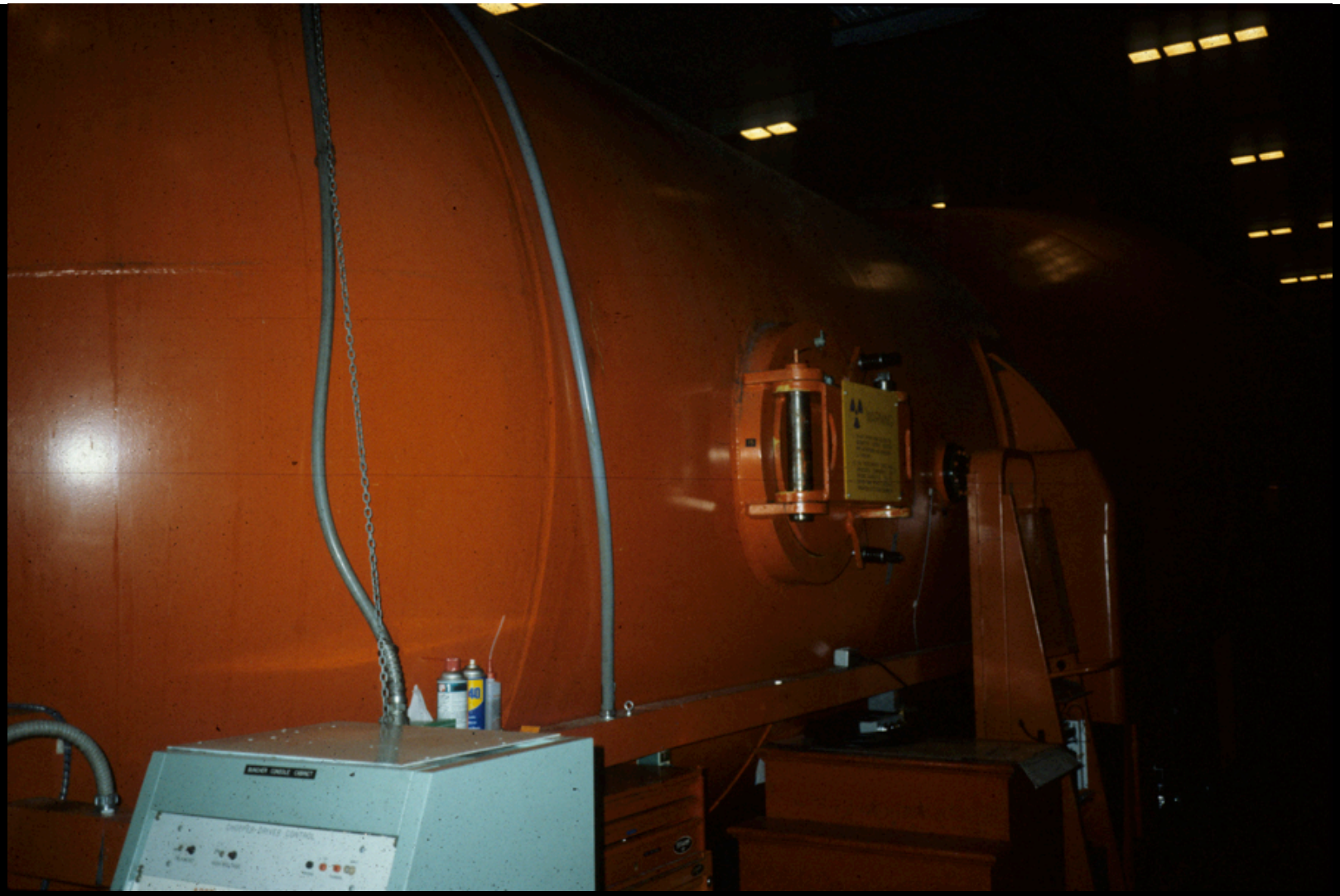

Improvement in accelerator mass spectrometry (AMS) have allowed geochronologists to directly measure the ^{14}C to stable carbon(^{12}C and ^{13}C) ratio. The ratio of ^{14}C to ^{12}C or ^{13}C will be reduced by 50% after one half-life. AMS ^{14}C dating requires a much smaller organic sample (milligrams versus grams) than the beta-counting method. Most ^{14}C analyses today are measured using AMS.

Source of Error in ^{14}C dating

1. Variations in geomagnetic flux. Geomagnetic field strength partly controls ^{14}C production in the atmosphere because of attenuation affects on the cosmic flux with increasing magnetic field strength.
2. Modulation of the cosmic-ray flux by increased solar activity (i.e., solar flares) leads to attenuation of the cosmic-ray flux.
3. Influence of the ocean reservoir. Any change in exchange rate between ocean reservoir and atmospheric reservoir will affect the level of ^{14}C in the atmosphere.
4. Industrial revolution (ratio of ^{14}C to stable carbon decreased because of burning fossil fuels) and bomb effects (^{14}C to stable carbon increased because of increased neutron production from detonation of nuclear bombs in the atmosphere) have made modern organic samples unsuitable for as reference samples.

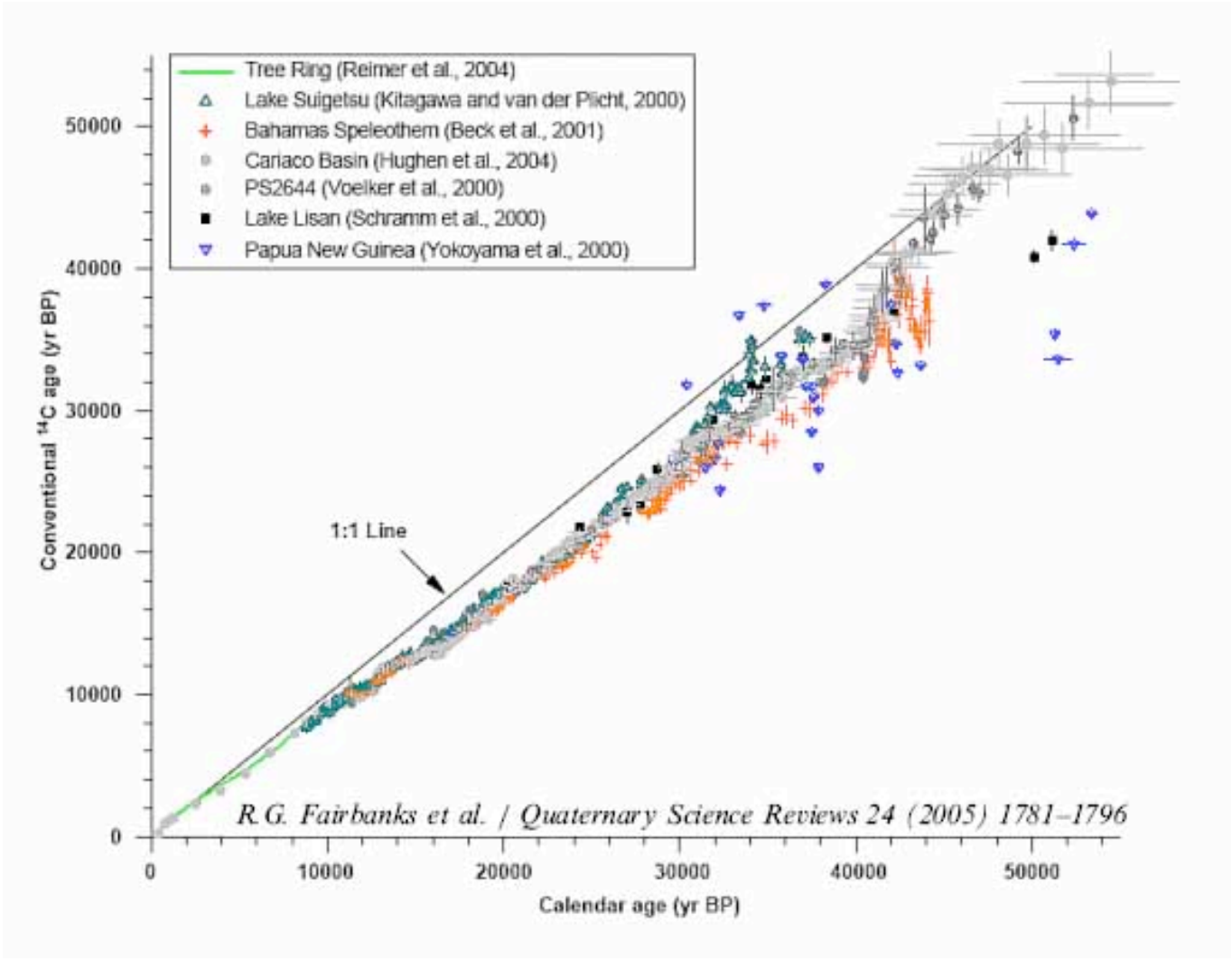

U-Th dating of corals has extended the ^{14}C calibration curve back to 50,000 years (Fairbanks *et al.,* 2005).

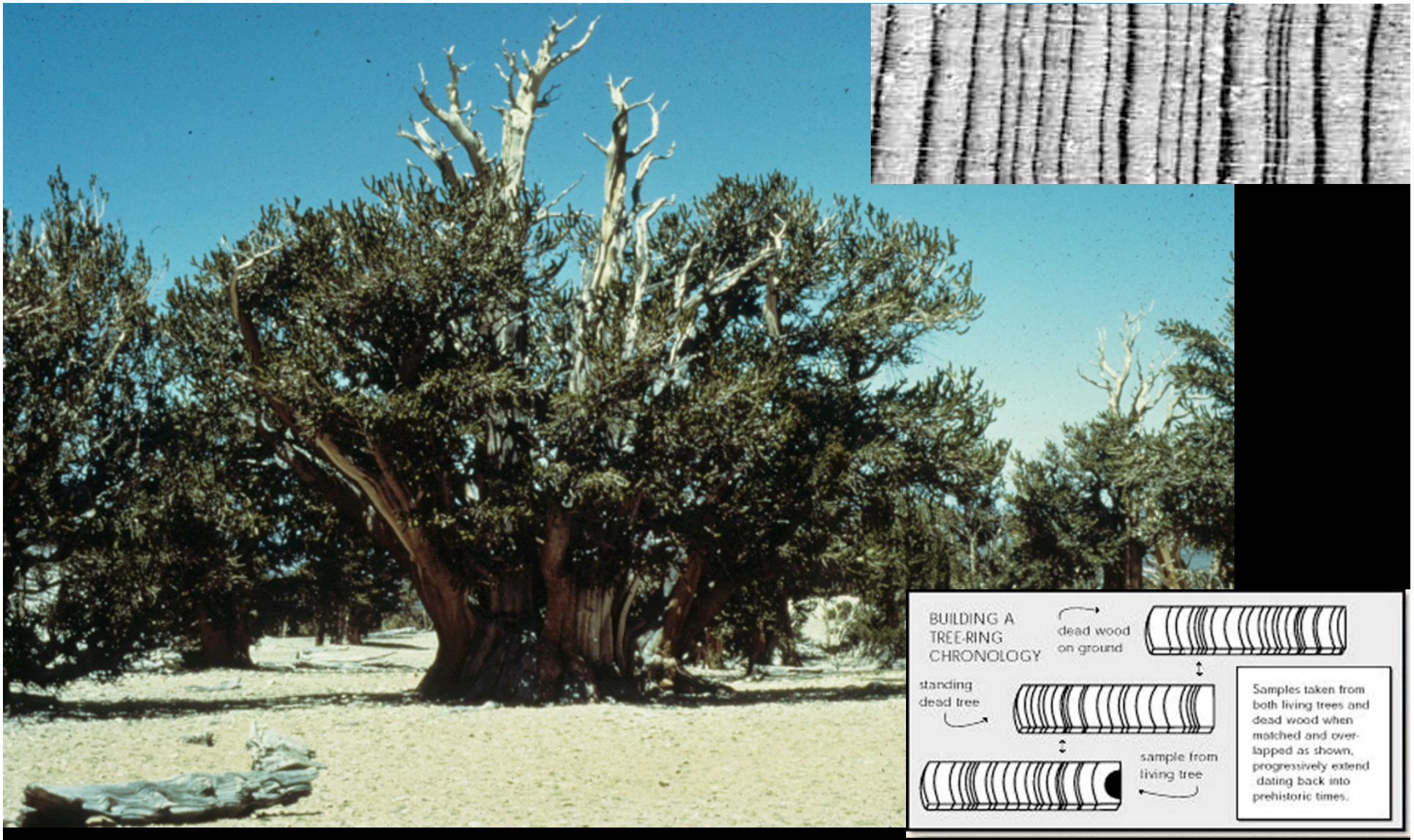

Dendrochronolgy (tree ring counting) has been useful for calibration of ^{14}C ages with calendar ages. Trees growing at latituded with seasonal variation in temperature will produce distinct growth rings during the spring-summer (light color) and fall-winter dark color). The bristlecone pine record in the White Mountains, CA has been extended back >10,000 years.

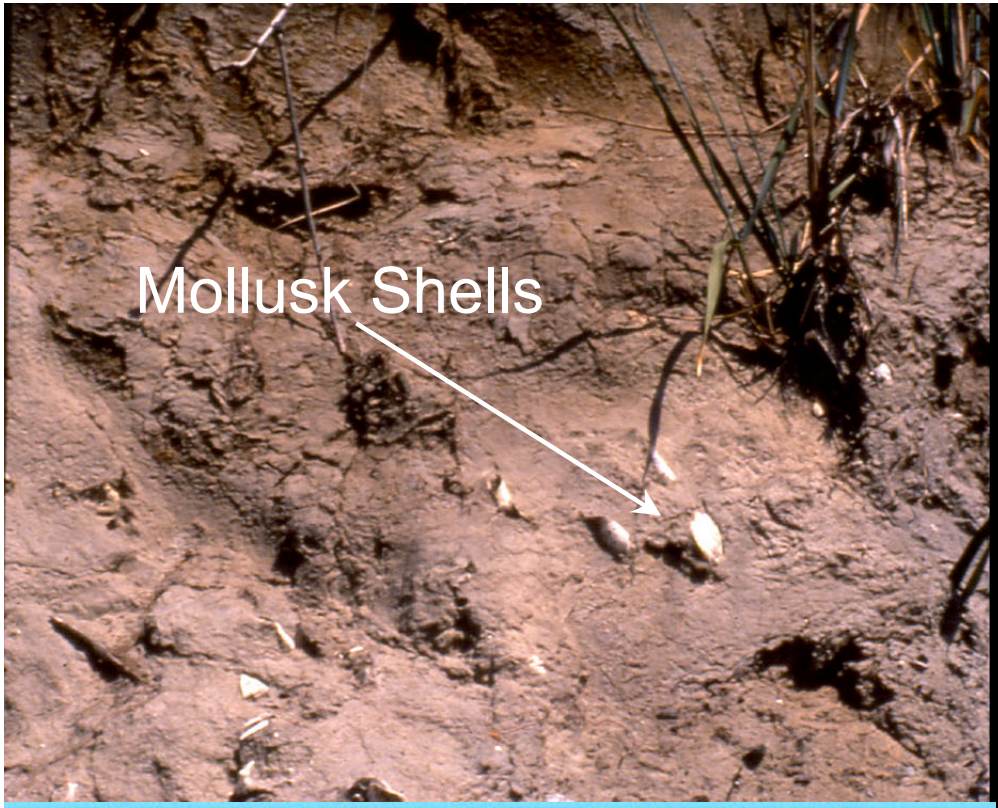

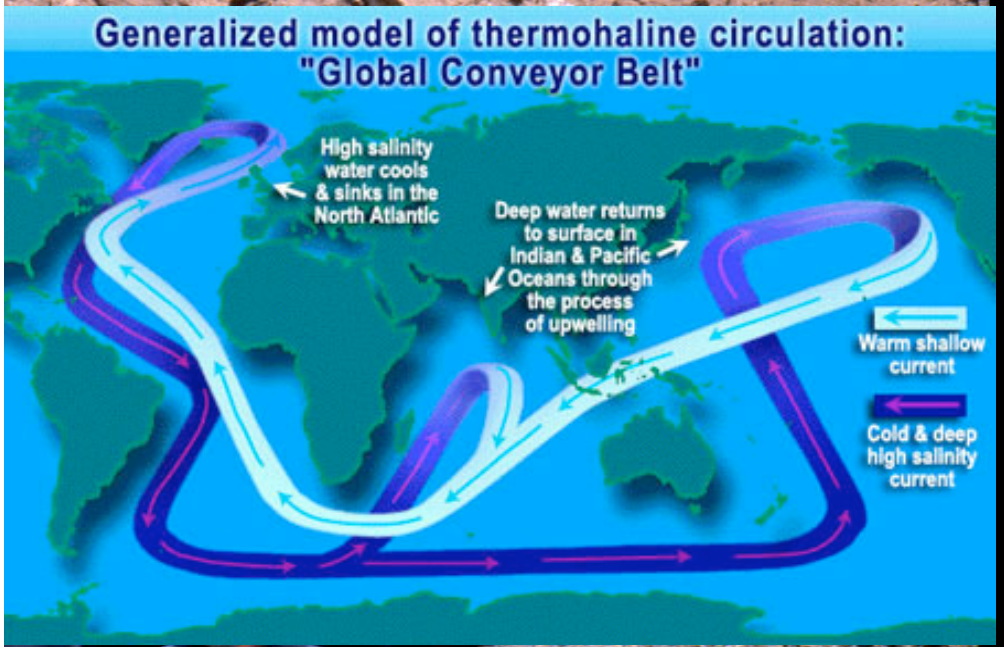

Marine Reservoir Effect

The radiocarbon age of marine carbonates will reflect the age of the carbon in the ocean reservoir.

Because deep ocean waters are slowly mixed with surface waters, the radiocarbon age reflects the residence time of the carbon within the water.

Deep water production in the North Atlantic slowly cycles to the Pacific where it upwells along the coastline of South America and North America. The residence time of this circulation is over 1000 years. Marine organisms living in this upwelling water will yield radiocarbon ages that are much older than the true age of the organism. The reservoir effect must be known to assess ^{14}C ages of marine shells in GMD.

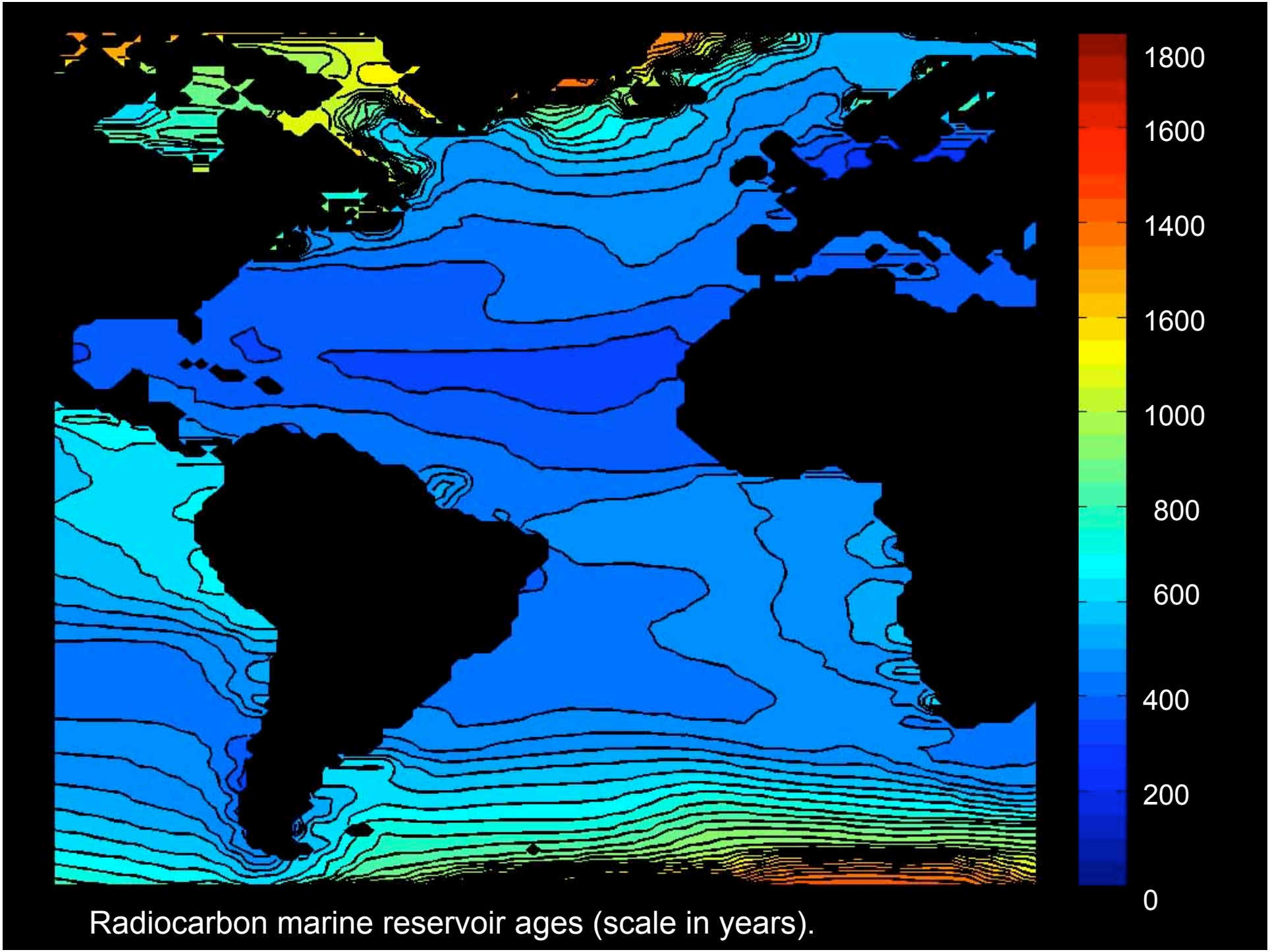

Radiocarbon marine reservoir ages (scale in years).

Radiocarbon dating is useful for assigning ages to sediment that may incorporate organics during erosion and deposition, such as this log present in glacial till.

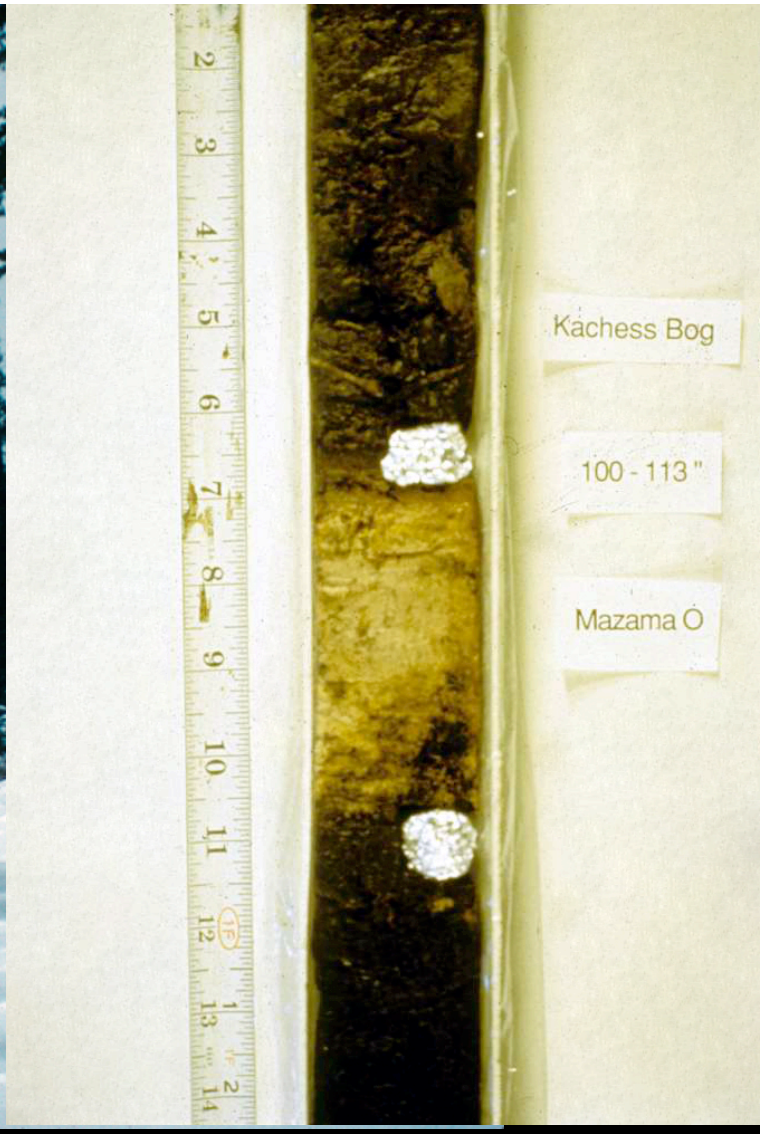

Radiocarbon dating is useful for assigning ages to young (<50,000 years old) volcanic ash layers, such as the Mazama (Crater Lake) tephra shown above. The above sediment core was collected from Kachess Lake, lying east of Snoqualmie Pass, WA.

Radiocarbon dating is useful for capturing illegal contraband, made from endangered species, such as this whale bone carving. Organic material that retains “bomb-effect” ^{14}C levels must post-date the 1950’s.

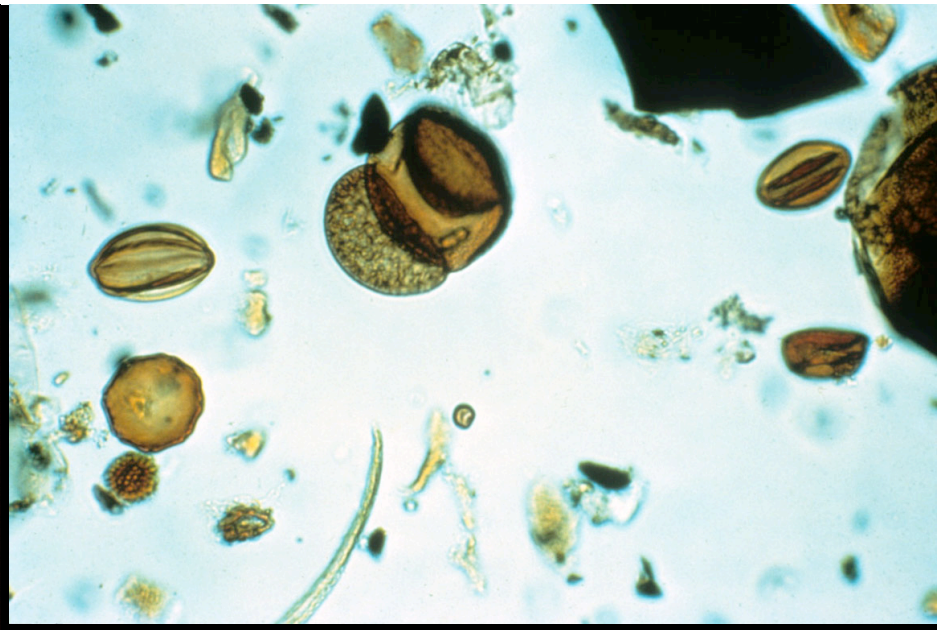

Radiocarbon dating has provided age constraints on the timing of vegetation change by dating organics in lake sediment collected by a Livingston core. Vegetation change, inferred from a fossil pollen record provides a proxy of climate change for a given region.

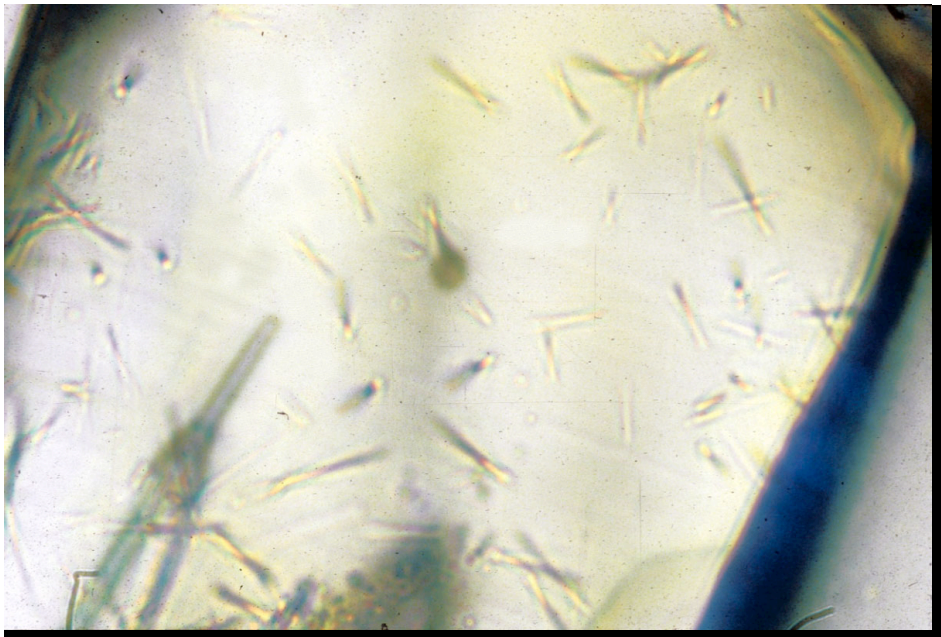

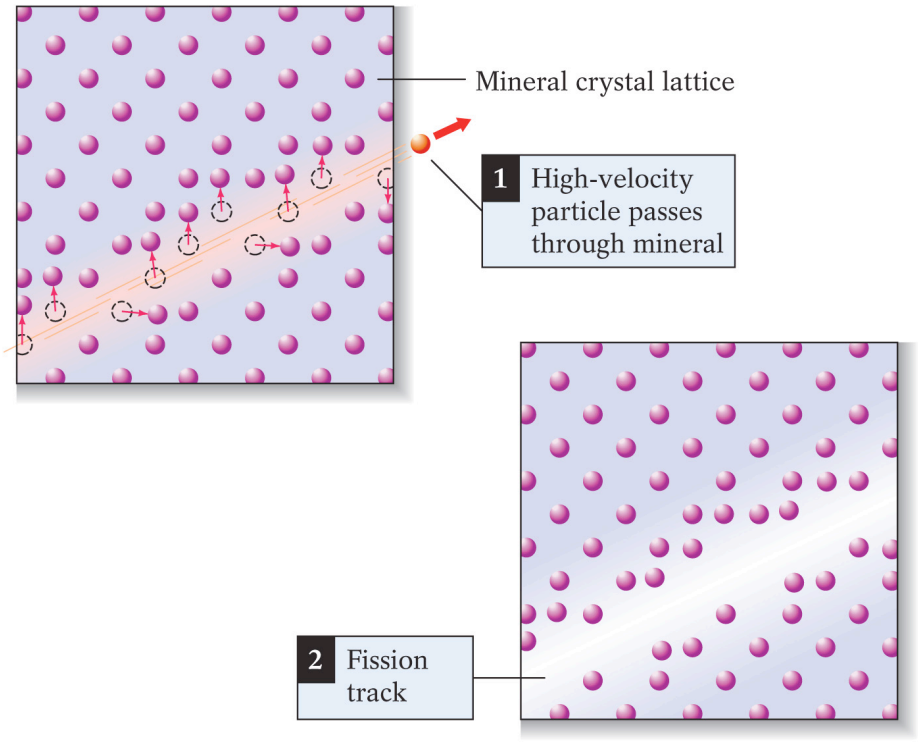

Fission Track Dating

Fission track dating is useful for dating U-bearing minerals (i.e., apatite, zircon or sphene) in felsic to intermediate igneous rocks.

Fission track dating is based on the premise that nucleus of ^{238}U atoms can also decay by spontaneous fission to atoms of intermediate atomic numbers (e.g., ^{56}Ba). During the fission process damage tracks are created as high-speed collisions occur between fission fragments and neighboring atoms.

The fission tracks can be preserved within the U-bearing minerals for millions of years. The number of tracks is directly dependent upon 1. The initial ^{238}U content and 2. the age of the sample. Fission track is useful for dating materials between 300 ka and 100 Ma.

Fission Track Dating

Fission track dating is useful for dating felsic lava flows or tephra layers that have ages that exceed 300,000 years. The fission track age of the Bishop Ash (718,000 years) provides a maximum limiting age for the alluvial fan deposit overlying it.

Fission tracks anneal (are erased) with heating and are therefore useful in dating uplift of igneous plutons, such as the Sierra Nevada mountains that have moved through the annealing temperature (200°C) during the uplift event.

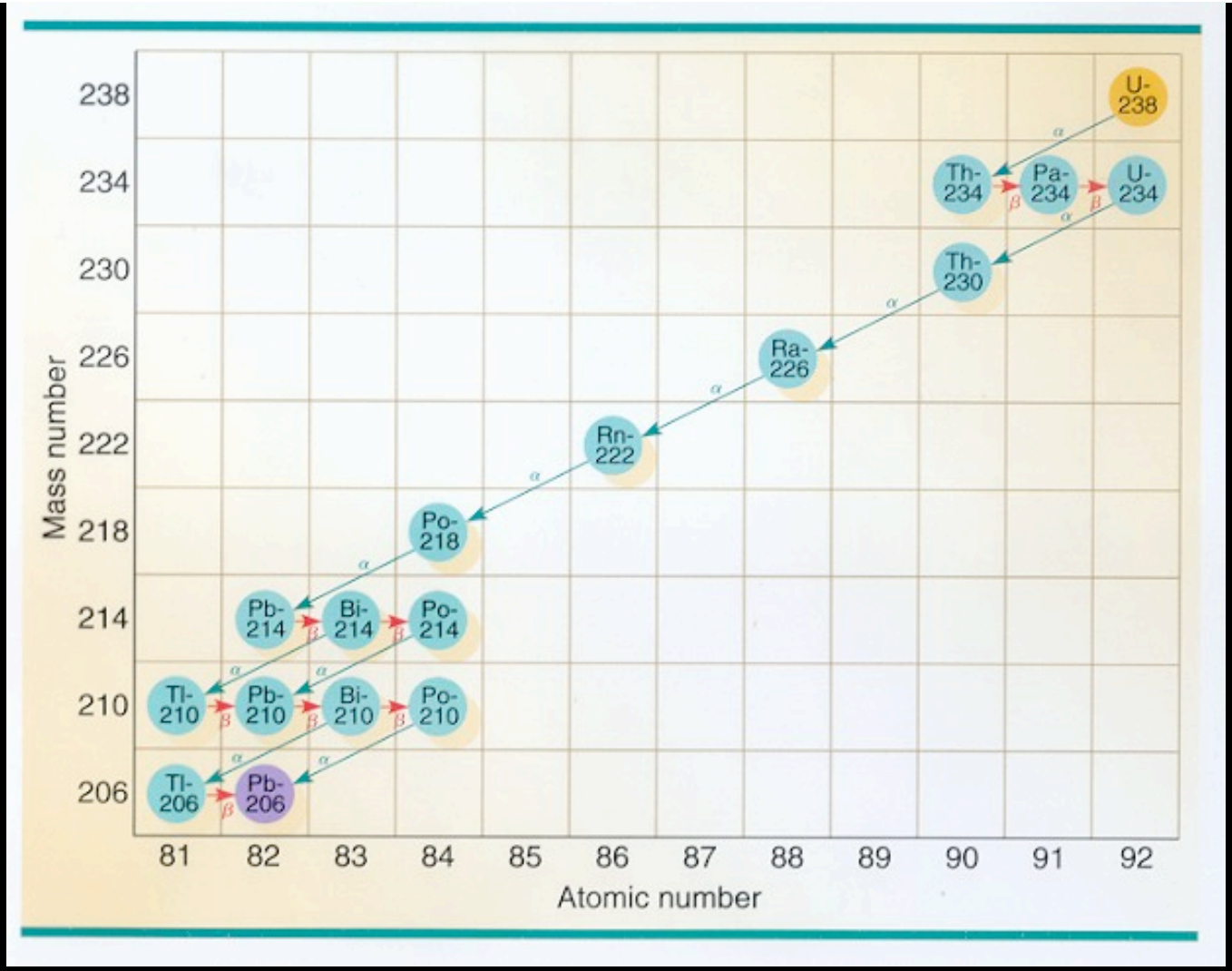

Uranium-series dating is based on the premise that the U-decay chain, that is typically in equilibrium (I.e., production rate of intermediate daughter nuclides is equal to their decay), is interrupted, where some decay products can be selectively removed from the system. When this occurs in nature, the U-decay series is in as state of disequilibrium and the removed isotope pairs can be used for dating.

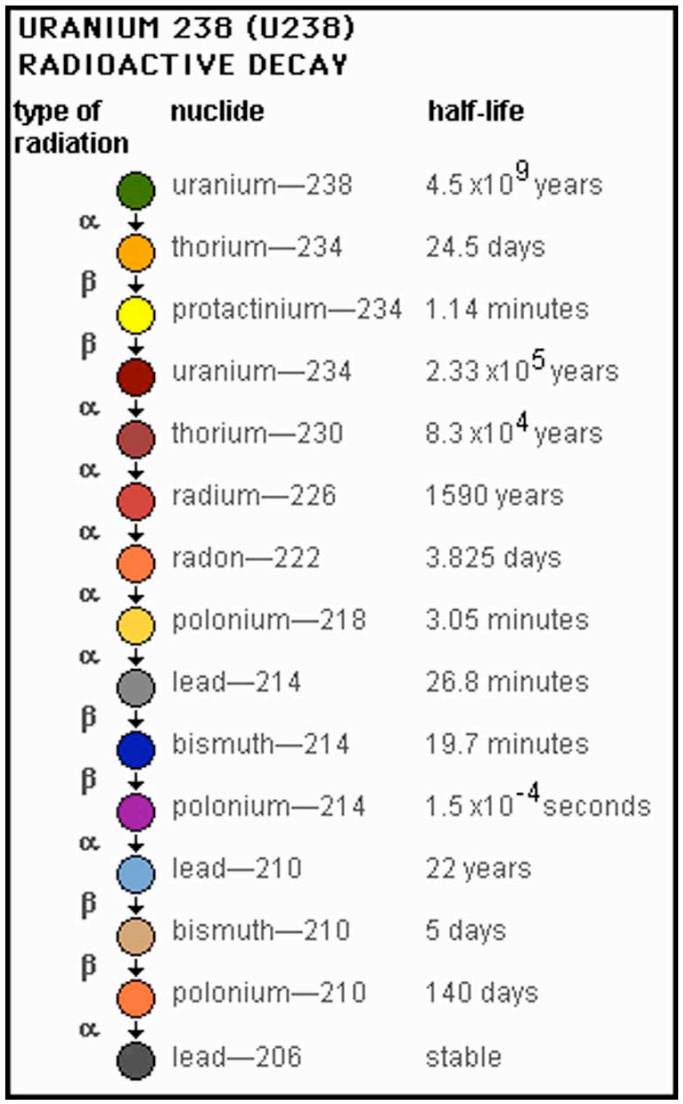

Uranium-series dating is based on the following geochemical principles: 1. Uranium and weathering products containing uranium are highly soluble and remain dissolved in water, whereas thorium and protactinium are readily absorbed or precipitated and contained within the sediment record.

Because of this disequilibrium the ^{234}U-^{230}Th isotope pair can be used to assign U-Th ages to organisms that secrete carbonate directly from ocean or lacustrine waters (such as coral reefs, tufa or mollusk shells). The half-life for this isotope pair is ~233,000 years and is applicable to Quaternary aged materials.

^{230}Th decays to ^{226}Ra with a half-life of ~83,000 years. Marine or lacustrine sediment can be dated up to 5 half-lives or 350,000 years.

U-Th ages of calcite tufa spires in Mono lake, California provide age constraints on the timing of the highest lake during the last glacial cycle (20,000 years ago. The paleo-lake level is seen as a beach terrace in distance.

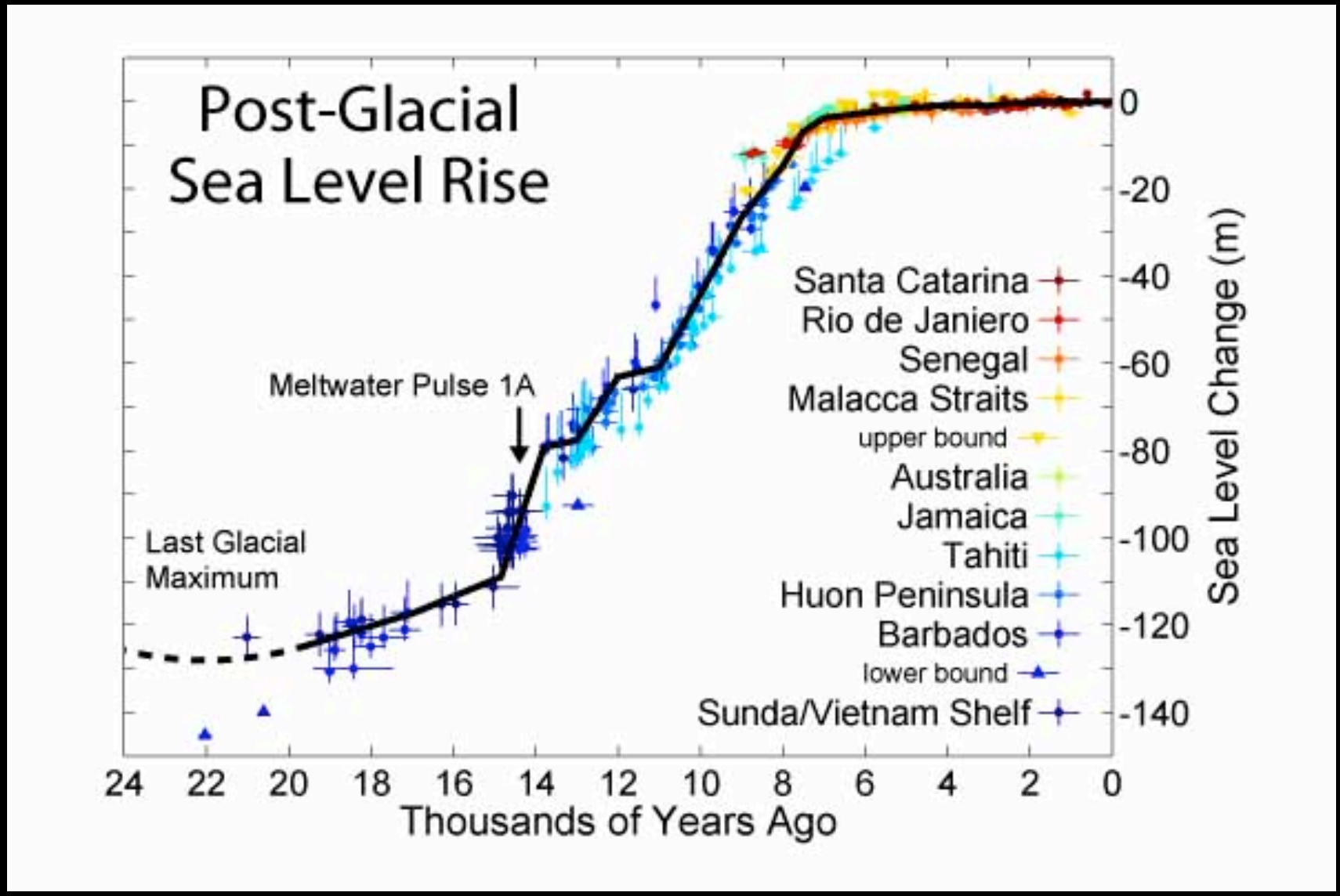

The post-glacial (eustatic) sea level rise was determined by U-Th dating of corals that lived at the existing sea level.

Thermoluminescence (TL) Dating

1. TL dating can be applied directly to quartz and feldspar mineral grains in fine sediment. It can provide numerical ages ranging from 100 to 1,000,000 years.
2. Radioactive isotopes (U, Th, K) in sediment constantly bombard minerals with alpha, beta and gamma particles, which damage the respective crystal lattice, displacing electrons into lattice defects.
3. Heating the sample to 500°C or exposure to sunlight for more than 8 hours releases the trapped electrons, producing TL (a light in addition to the incandescent glow of heated materials). The radiation record is erased (bleached) and the TL clock is set to zero.
4. The strength of the measured TL signal is dependent upon trapped electrons, which is a function of time and natural radiation dose.

Thermoluminescence (TL) Dating

TL may be used to determine the elapsed time since a given sample was reset to zero by a thermal event (e.g., firing pottery, ceramics, tephra or sediment baked by lava flows), crystallization (e.g., biological and chemical precipitation), or sun bleaching prior to deposition or burial (e.g., loess, dune sand, ocean sediments, lacustrine sediments).

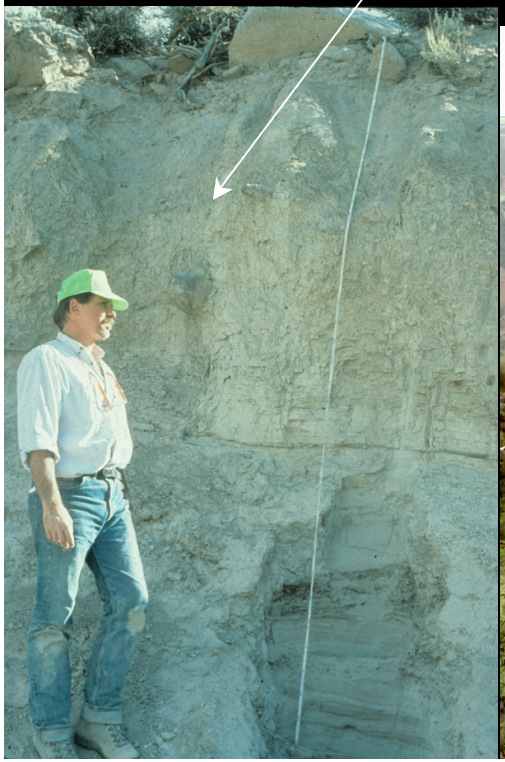

TL dating has been used to date pottery shards associated with human occupation sites (centuries to millenia time scales). The TL age is set at the time of firing of the pottery.

TL Ages are calculated using the following equation:

TL age (years) = $\frac{\text{TL acquired}}{\text{TL acquistion/year}} = \frac{\text{natural TL - residual TL}}{\text{(TL/unit rad dose X rad dose/year}}$

Natural TL measure by heating sample and photoelectronically counting the photons emitted during TL.

Residual TL (at zero age) is determined from modern surface samples or in the laboratory.

TL/unit radiation dose is the induced TL obtained by exposing the sample to a known radiation dose in the laboratory.

Radiation dose/year may be determined by direct measurement using dosimeters or chemical properties of the radioactive isotopes.

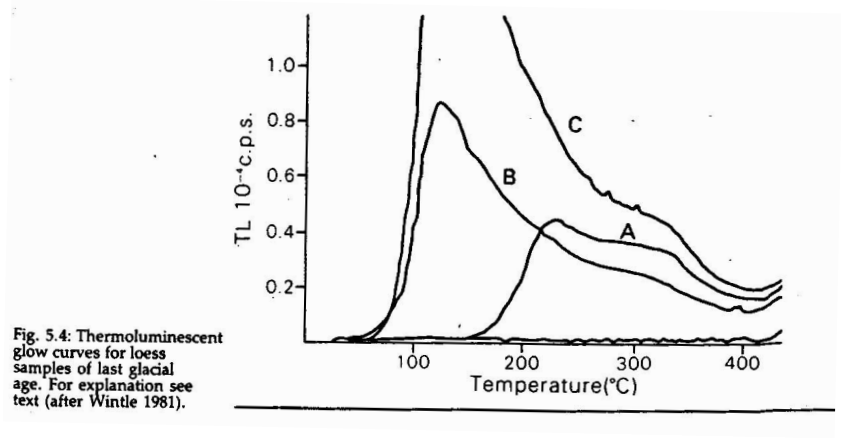

Fig. 5.4: Thermoluminescent glow curves for loess samples of last glacial age. For explanation see text (after Wintle 1981).

TL glow curves of loess samples measured in the laboratory.

Inherent Problems with TL Dating

1. TL growth is non-linear.
2. Zeroing may be incomplete, especially for water-lain sediment.
3. Water in sediment may absorb part of the radiation dose.
4. Radiation dose could change due to post-depostional processes, such as compaction or leaching.

Cosmogenic Isotope Dating

Glacial landforms, such as the Sierra Nevada moraines shown above, are difficult to date because of the absence of datable material and the fact that many numerical dating techniques are not applicable to age ranges between 50,000 and 300,000 years old. With improvements in AMS technology cosmogenic isotope dating has provided new opportunities for dating landforms that in the past could only have relative age assignments

Cosmogenic Isotope Dating

Cosmogenic isotopes are produced in near surface rock by collisions of high energy neutrons with specific target elements in rock.

Cosmogenic isotopes are largely produced in terrestrial deposits near the surface of the earth because the cosmic flux is attenuated by rock at depths that exceed 2 m.

Providing the production rate of a given cosmogenic isotope is known, as well as it decay constant or half-life (for radioactive isotopes) the exposure age can be determined using the following equation:

$$T = \frac{\ln(1 - N\lambda/P)}{-\lambda}$$ assuming no erosion

Where, T is the length of irraditation, N is the number cosmogenic produced atoms, λ is the decay constant, and P is the cosmogenic isotope production rate.

Cosmogenic Isotope Dating

Commonly measured cosmogenic nuclides in rock.

Isotope	Half-life (yr)	Target Elements	Production Rate (atoms $g^{-1}yr^{-1}$)
^{3}He	stable	O,Si,Mg,Fe,Al	100-150
^{21}Ne	stable	Si,Mg,Fe,Al	80-160
^{10}Be	1.5×10^{6}	O,Si,Mg,Fe,Al	6-8 (quartz)
^{26}Al	7.2×10^{5}	Si,Mg,Fe,Al	37
^{36}Cl	3.0×10^{5}	K, Ca, Cl	8-10 (basalt)
^{14}C	5.7×10^{3}	O,Si,Mg,Fe	20

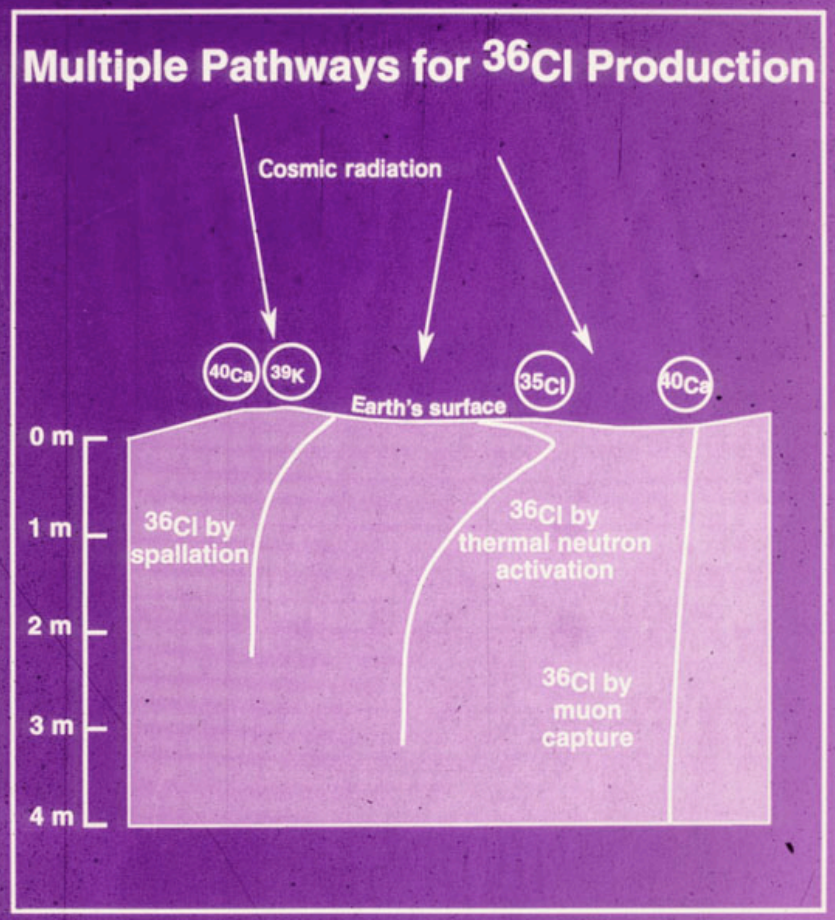

Production of 36Cl in Rock

Cl-36 is produced in earth rock via three major production pathways: spallation reactions with ^{40}Ca and ^{39}K, neutron activation of 3^5Cl and minor production via muon capture of ^{40}Ca.

Cl-36 Production in rock can be expressed by the following simplified equation:

$$P = \psi_{Ca}(C_{ca}) + \psi K(C_K) + \psi n\ (\sigma_{35}N35/\Sigma\sigma_i N_i),$$

Where, ψ_{Ca} and ψ_K are the total production rates of 36Cl due to C and K, C_{ca} and C_K are the elemental concentrations of C and K, ψn is the thermal neutron capture rate, which is dependent upon the fraction of neutrons stopped by ^{35}Cl ($\sigma_{35}N35/\Sigma\sigma_i N_i$), as determined by the effective cross sections of ^{35}Cl (σ_{35}) and all other absorbing elements ($\Sigma\sigma_i$) and their respective abundances (N_{35} and N_i).

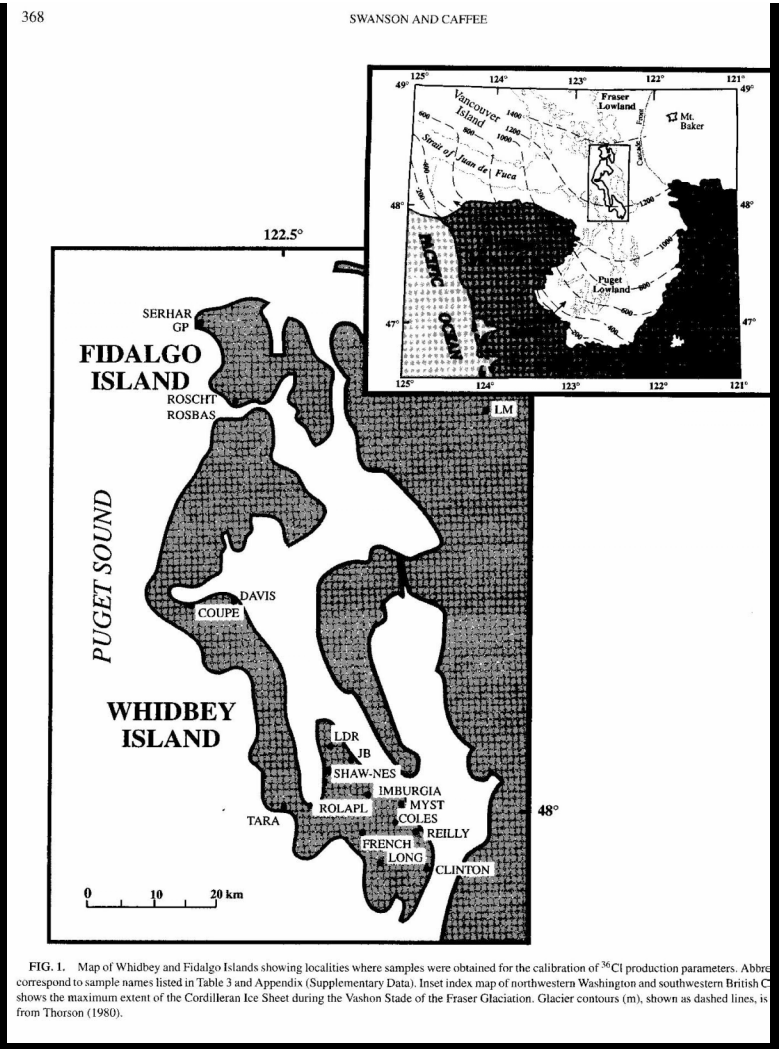

FIG. 1. Map of Whidbey and Fidalgo Islands showing localities where samples were obtained for the calibration of ^{36}Cl production parameters. Abbre correspond to sample names listed in Table 3 and Appendix (Supplementary Data). Inset index map of northwestern Washington and southwestern British C shows the maximum extent of the Cordilleran Ice Sheet during the Vashon Stade of the Fraser Glaciation. Glacier contours (m), shown as dashed lines, is from Thorson (1980).

Whidbey and Fidalgo Islands provided excellent calibration sites for determination of the ^{36}Cl production rates. Exposed bedrock and large till boulders are composed of diverse lithologies and the deglaciation history (i.e., timing of exposure) is well-dated.

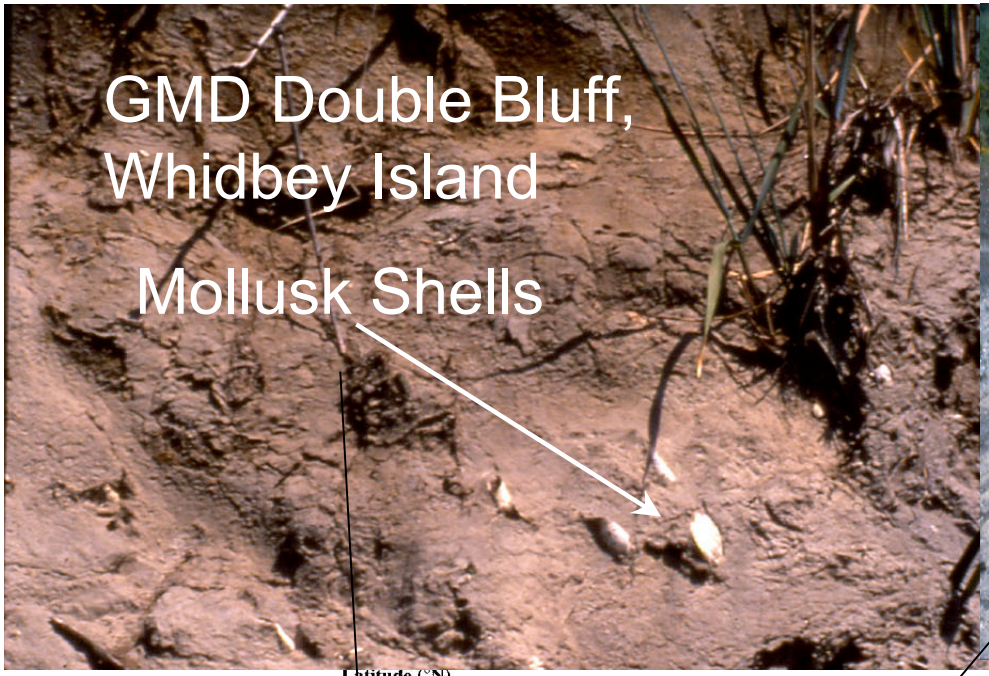

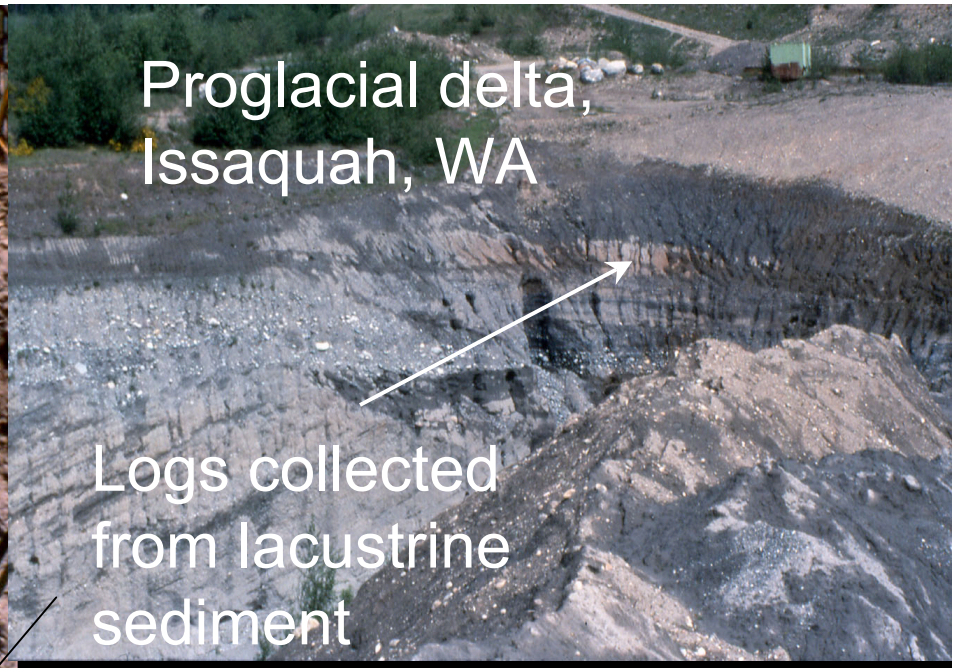

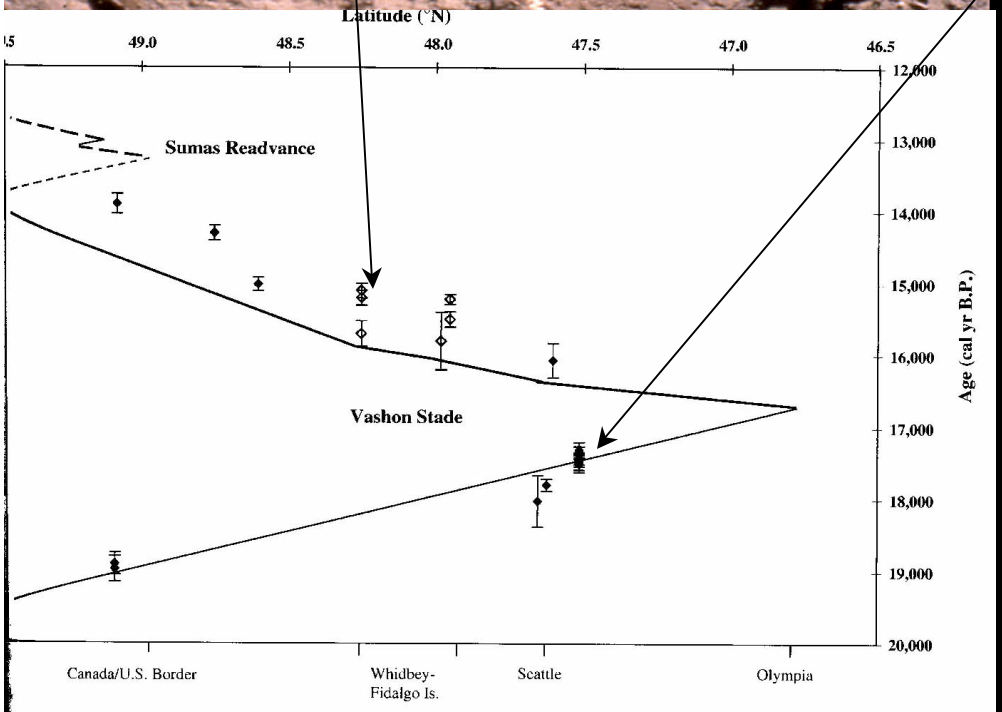

G. 2. Time–distance diagram showing the chronology of advance and retreat of the Cordilleran Ice Sheet into the Puget and Fraser Lowlands as constrained ge limiting ^{14}C ages. The ^{14}C ages used to construct this chronology are taken from Table 2. A 400-yr ^{14}C reservoir effect was assumed for glacialmarine ell ages (shown as open diamonds).

The deglaciation history of the Puget Lowland is well constrained by many wood and GMD shell ages under- and overlying the Vashon Till. Whidbey Island is inferred to have been deglaciation ~15,200 cal. yr ago.

The diverse bedrock geology within the accumulation area of the Puget Lobe ice sheet provides a diverse suite of target elements within the exposed till boulders. Certain lithologies permitted individual target elements to be isolated and production rate calculations simplified (one unknown).

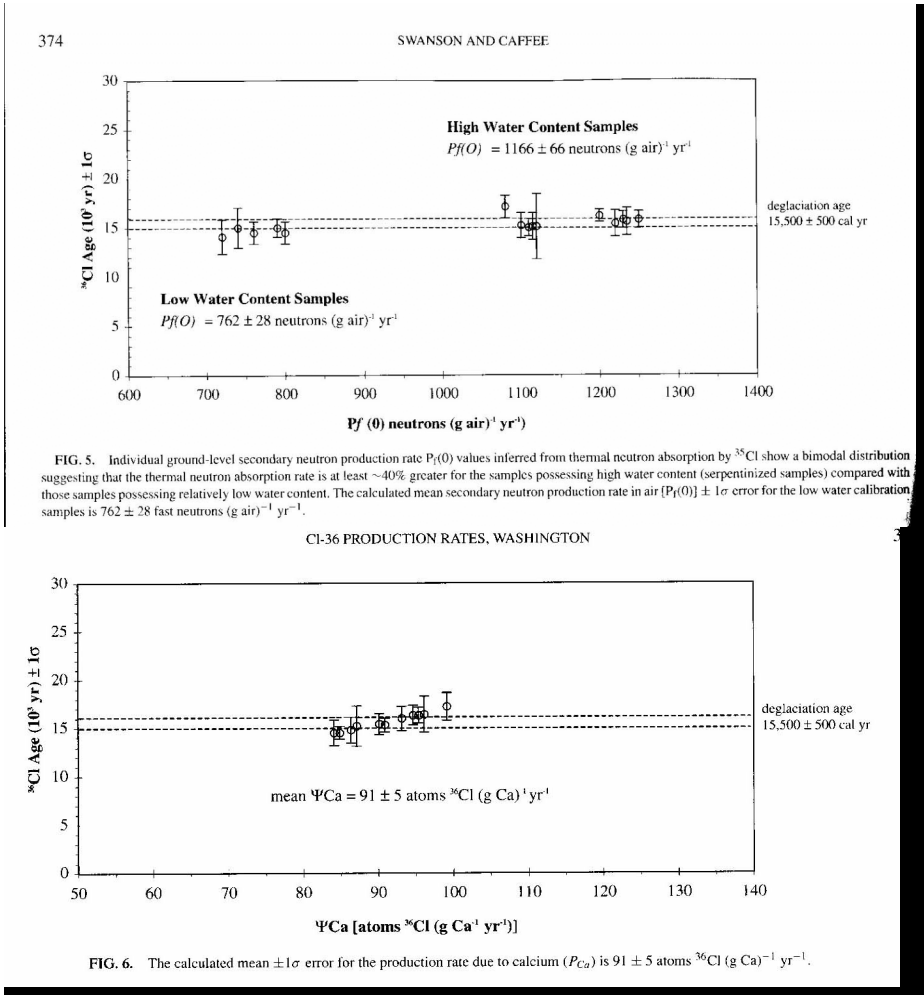

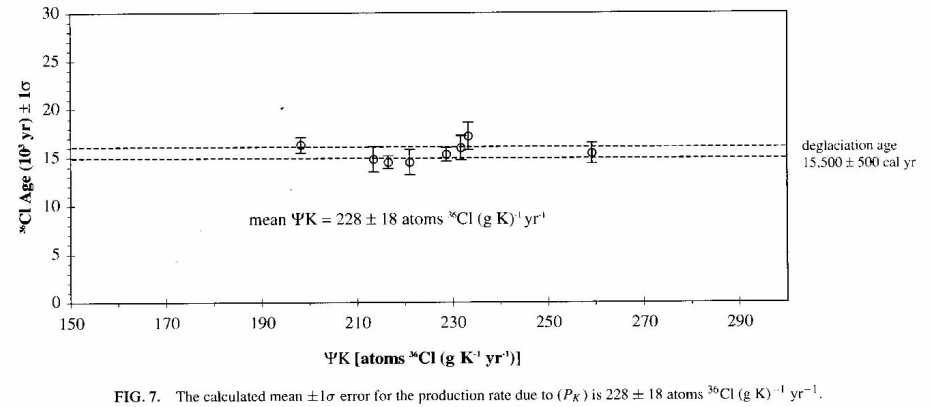

Cl-36 Production Rates

Because of the diverse lithology of the till boulders and bedrock surfaces in the study area, ^{36}C production pathways (^{35}C, ^{40}Ca and ^{39}K) could be isolated and the production rate for each target element solved with only one unknown. Previous calibration studies have relied on an iterative solution with multiple unknowns.

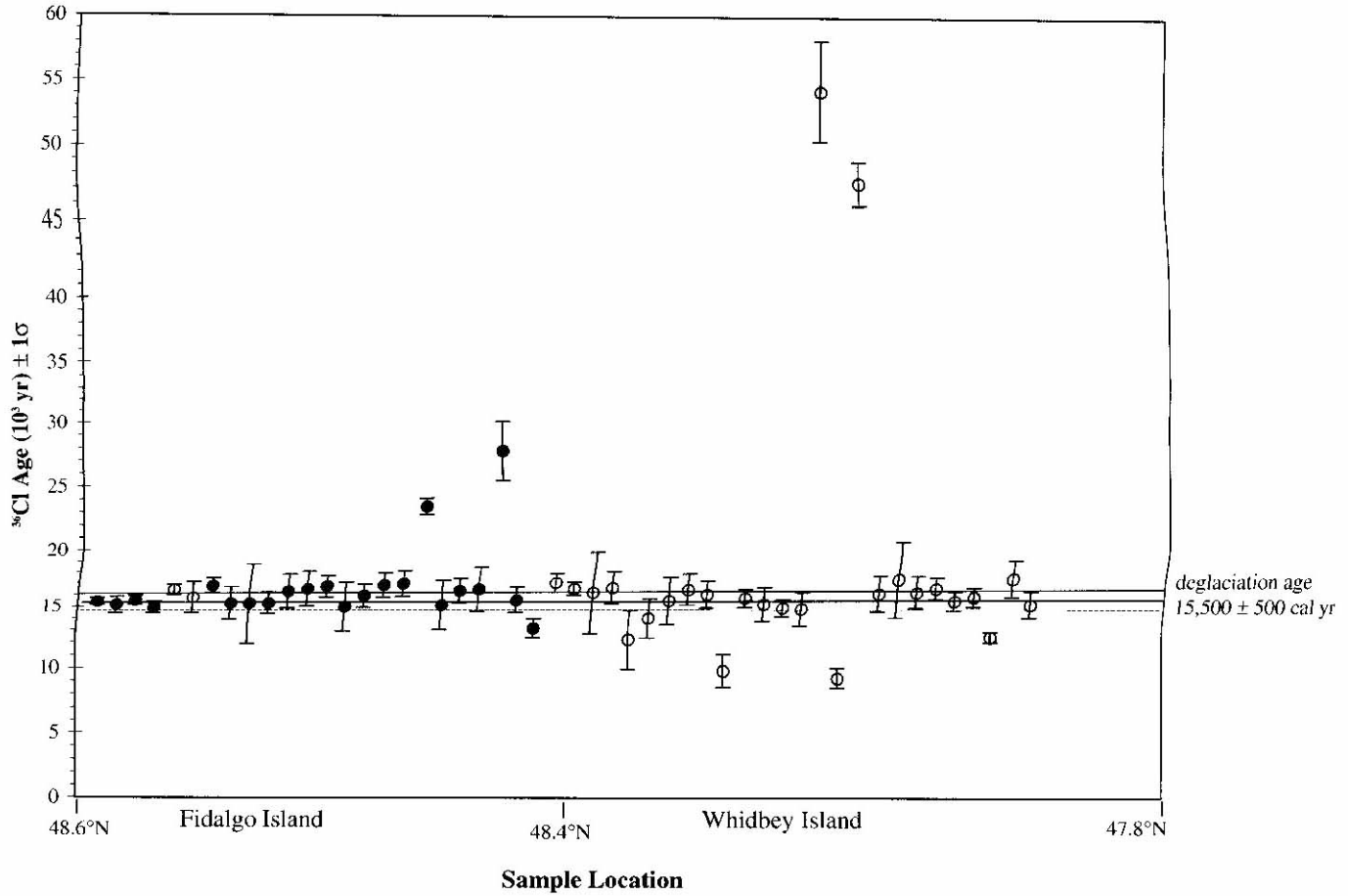

FIG. 8. Distribution of ^{36}Cl ages for all samples collected from Whidbey and Fidalgo Islands using the derived production rates. Statistical outliers are included and are also listed in the lower section of Table 3 and designated with the letters "s.o." Bedrock and erratic boulder samples are shown as filled and open circles, respectively.

Cl-36 ages of all samples collected from Whidbey Island using the calculated production rates of Swanson and Caffee (2001).

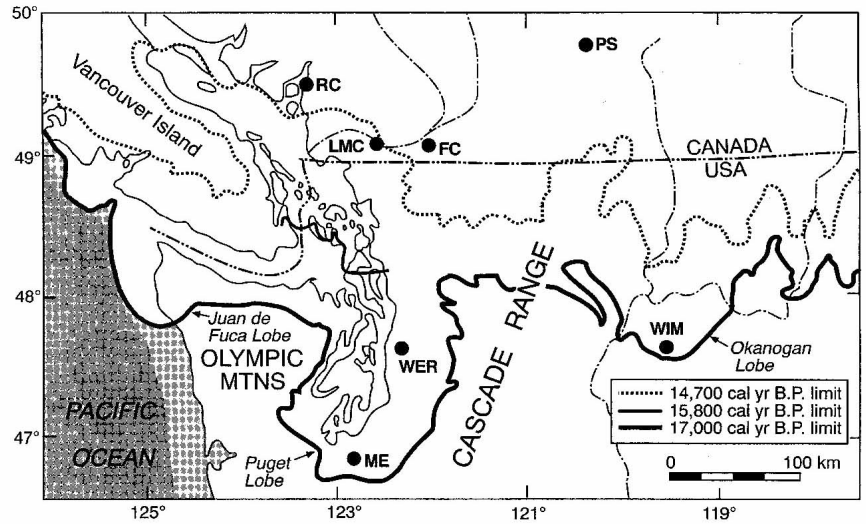

FIG. 9. Map showing the terminal position of the Cordilleran Ice Sheet at different times during the recessional phase of the Fraser Glaciation. Ice limi reconstructions taken from Clague *et al.* (1988) and Porter and Swanson (1998). Light-gray shading shows the inferred last glaciation emerged coast line. Location of the sample sites (including Ring Creek dacite flow) used to test the validity of the ^{36}Cl production rates are designated by their respective sample abbreviations

Validation of the ^{36}Cl production rates can be tested using other well-constrained glaciated surfaces in northern Washington and southern British Columbia.

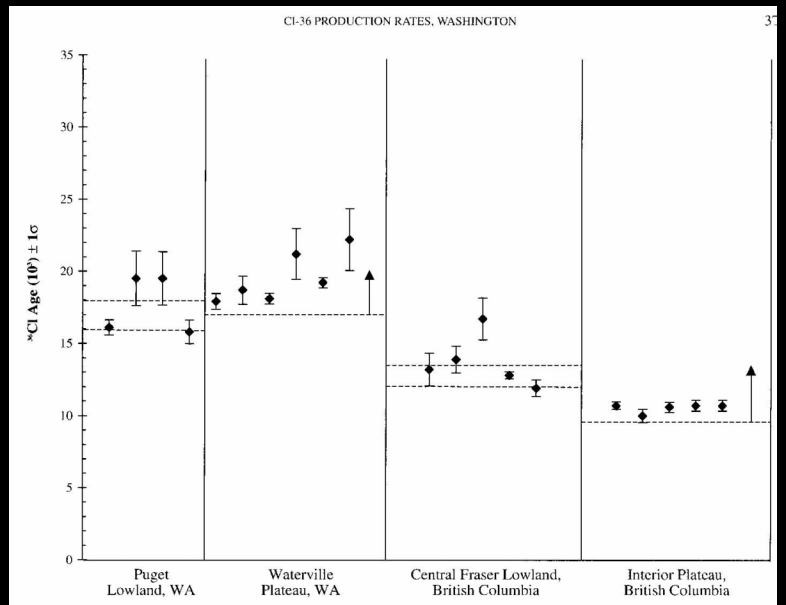

FIG. 10. Distribution of ^{36}Cl ages grouped according to their respective locations within the recessional limits of the Cordilleran Ice Sheet. The ^{36}Cl ages a consistent with independent radiocarbon ages constraining the timing of deglaciation at each location (bracketing calibrated ^{14}C ages are shown as two dash lines; minimum limiting ages are shown as a single dashed line and arrow), supporting the validity of the production rates reported here. These data are furth supported by the consistency of the calculated ^{36}Cl exposure age, using our production rates, and ^{14}C constraints for the eruption of Ring Creek dacite flow ne Squamish, British Columbia (discussed in text).

Haystack till boulder near Withrow, WA.

Boulder Frequency vs Moraine Age

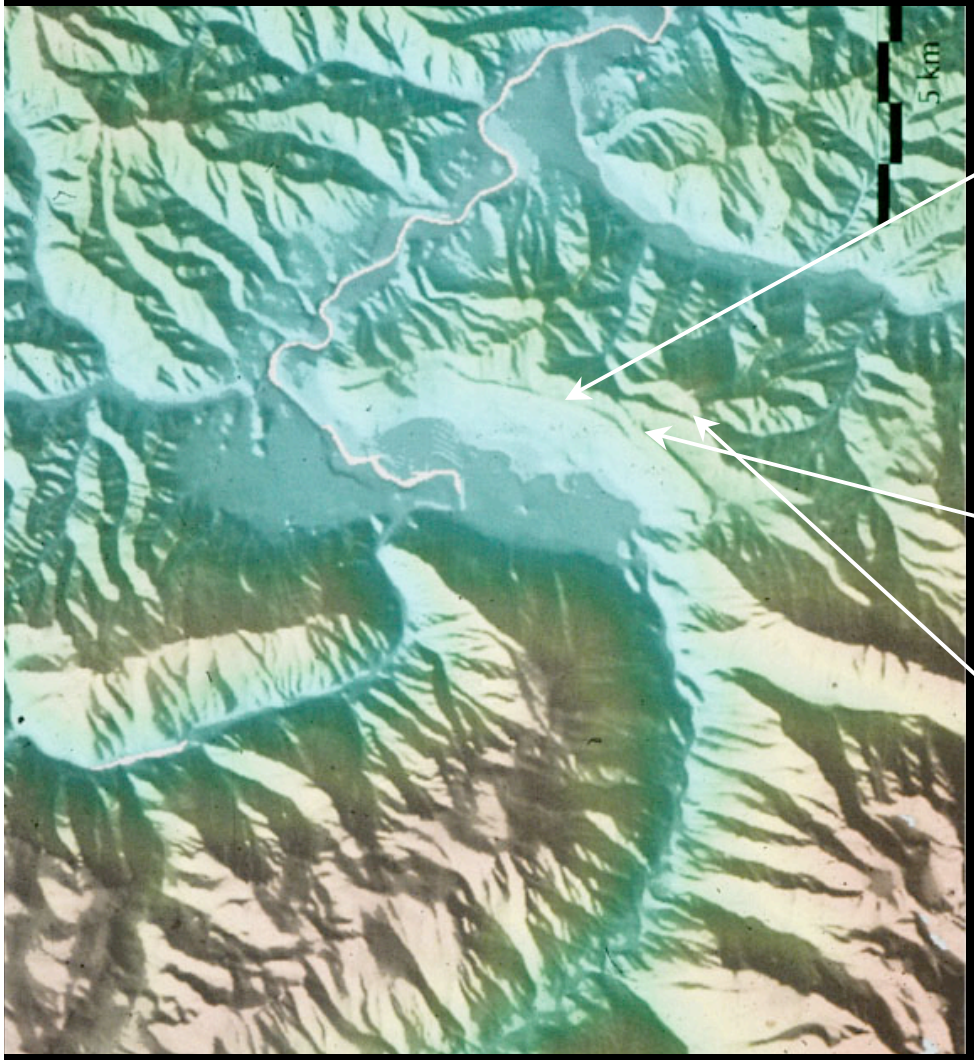

Stratigraphic position of moraine sequence in the Icicle Creek drainage, WA and boulder frequency count (from youngest to oldest moraines (top to bottom images).

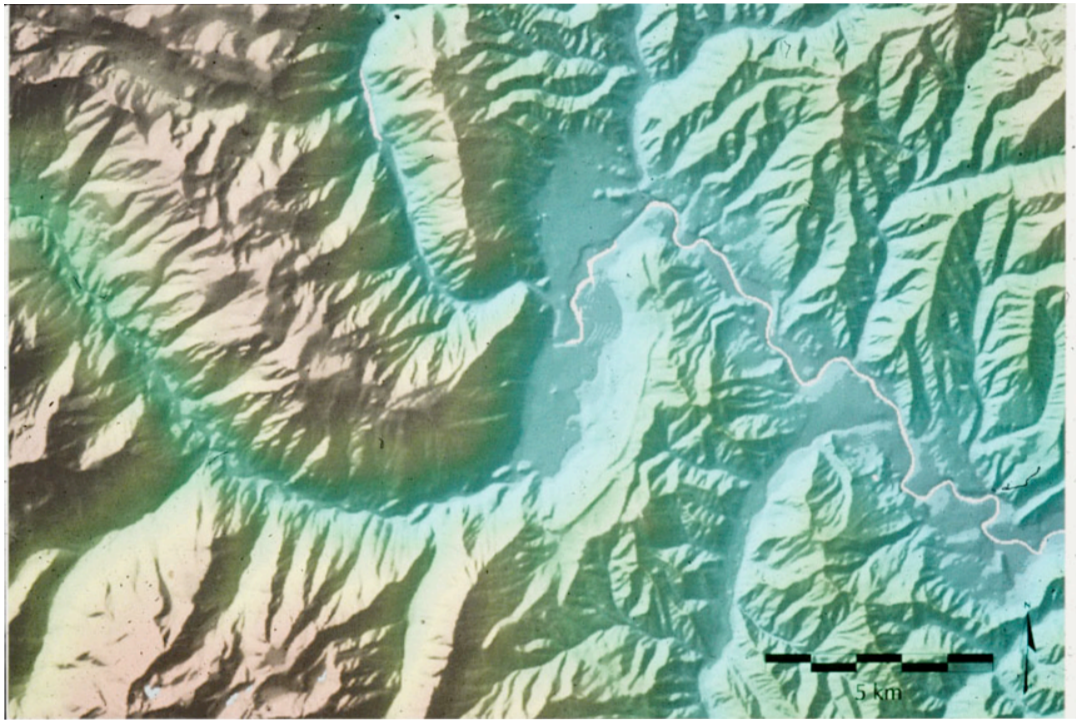

Cl-36 dating has been used to provide numerical age dating of the Icicle Creek moraine sequence near Leavenworth, WA.

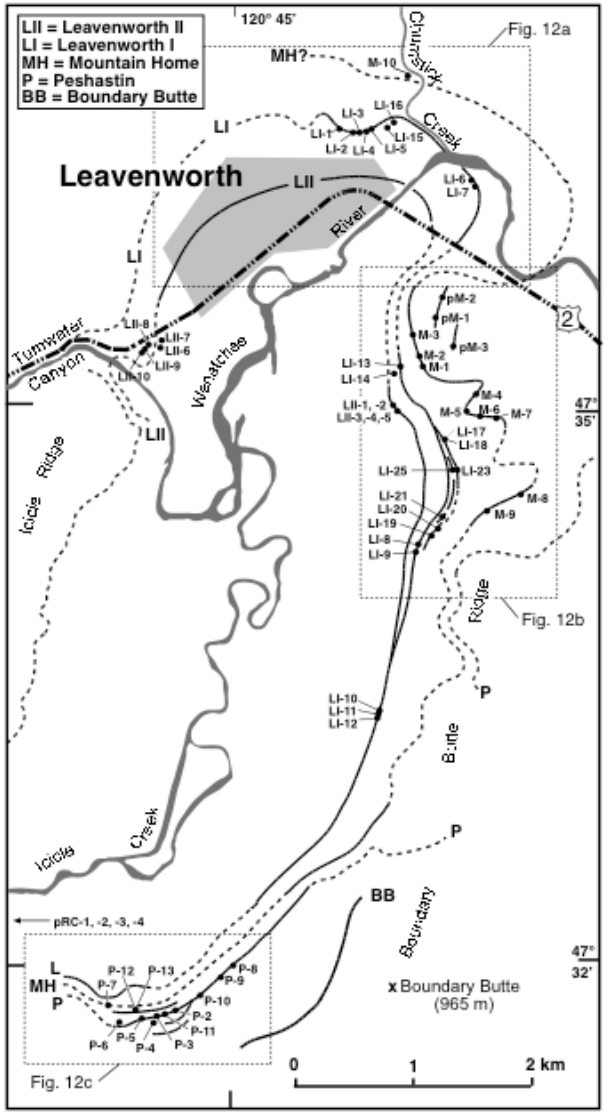

Porter & Swanson, Figure 10

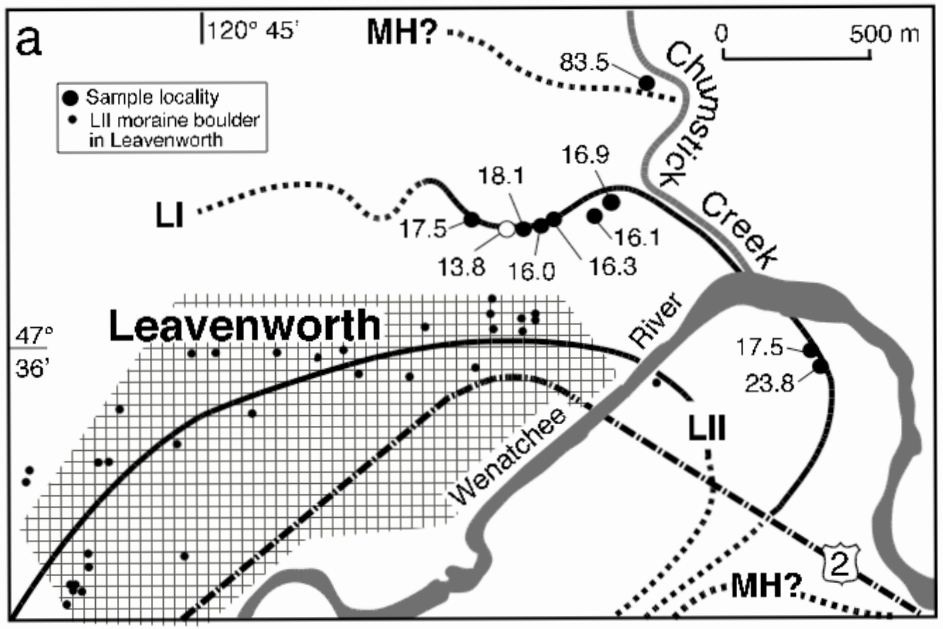

Porter and Swanson, Fig. 12a

CI-36 ages reported in (10^3 yr).

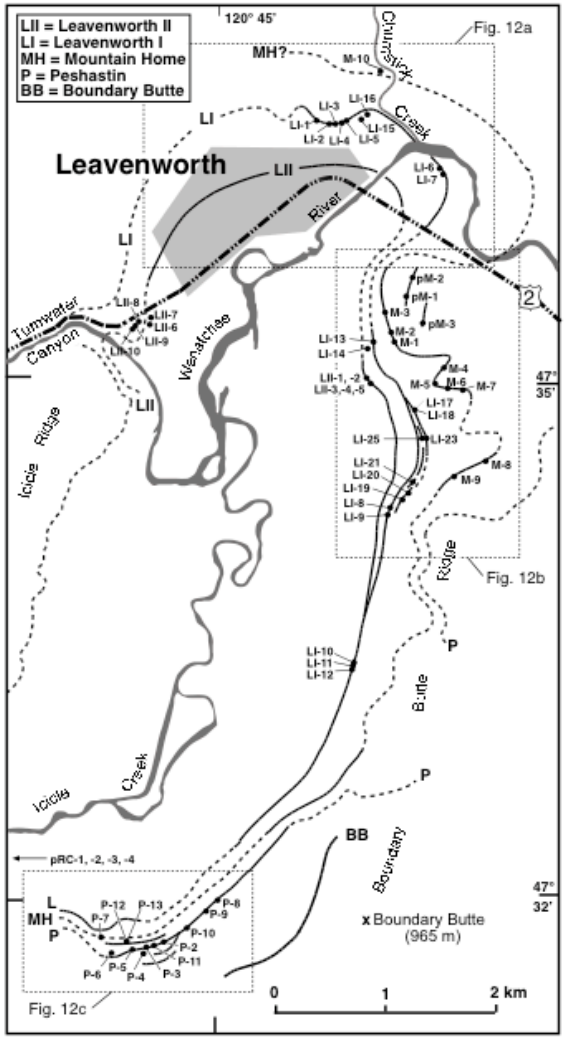

Porter & Swanson, Figure 10

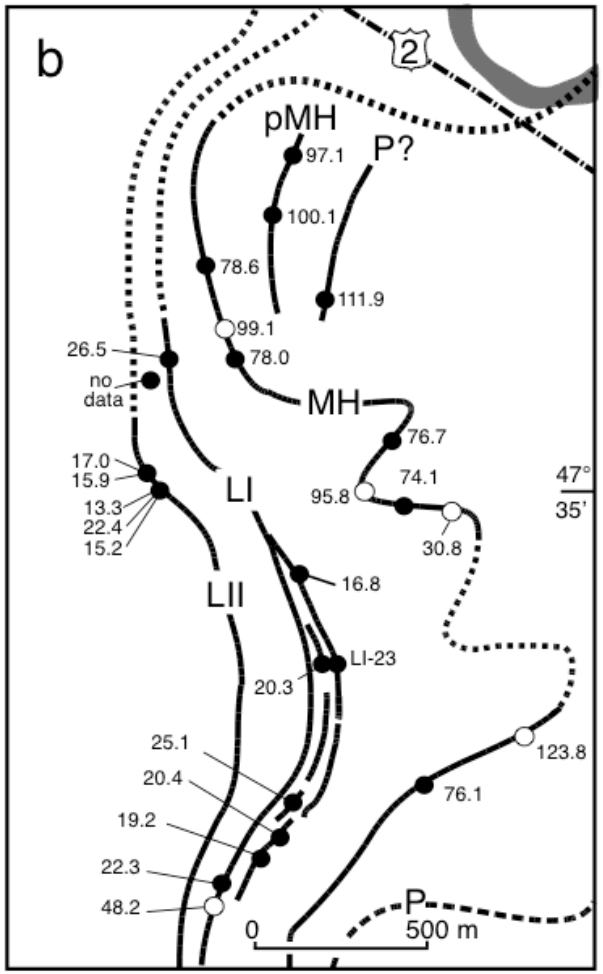

Porter and Swanson, Fig. 12 b

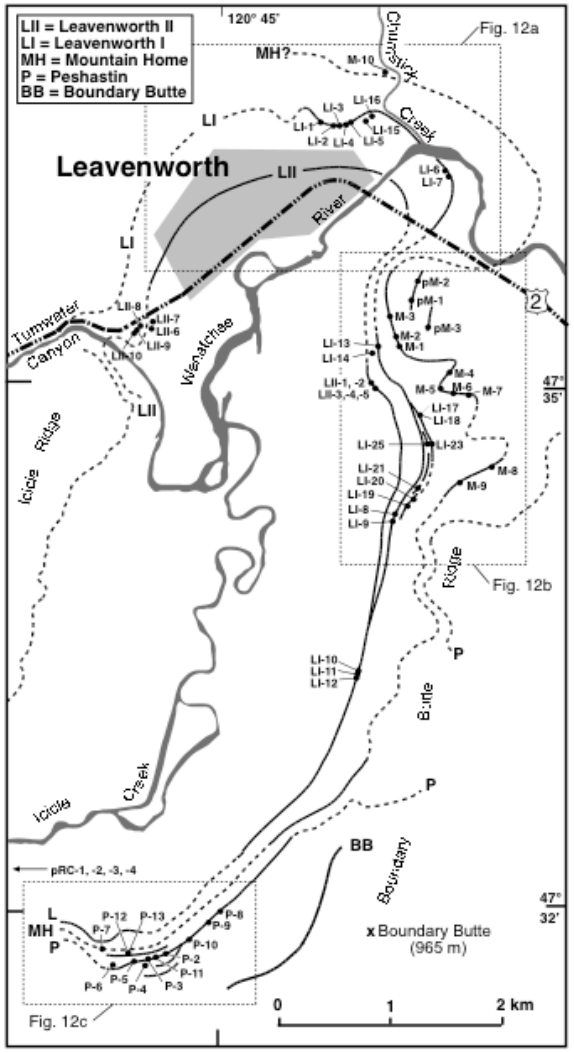

Porter & Swanson, Figure 10

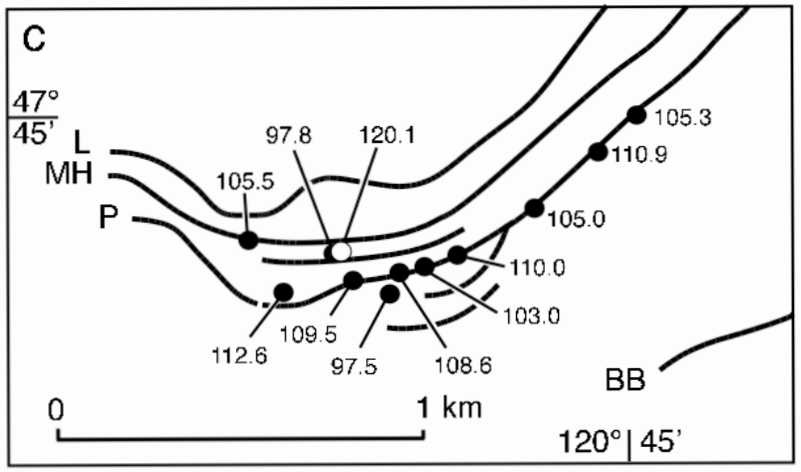

Porter and Swanson, Fig. 12c

The Peshastin moraines have ^{36}Cl ages that date to MIS 5d.

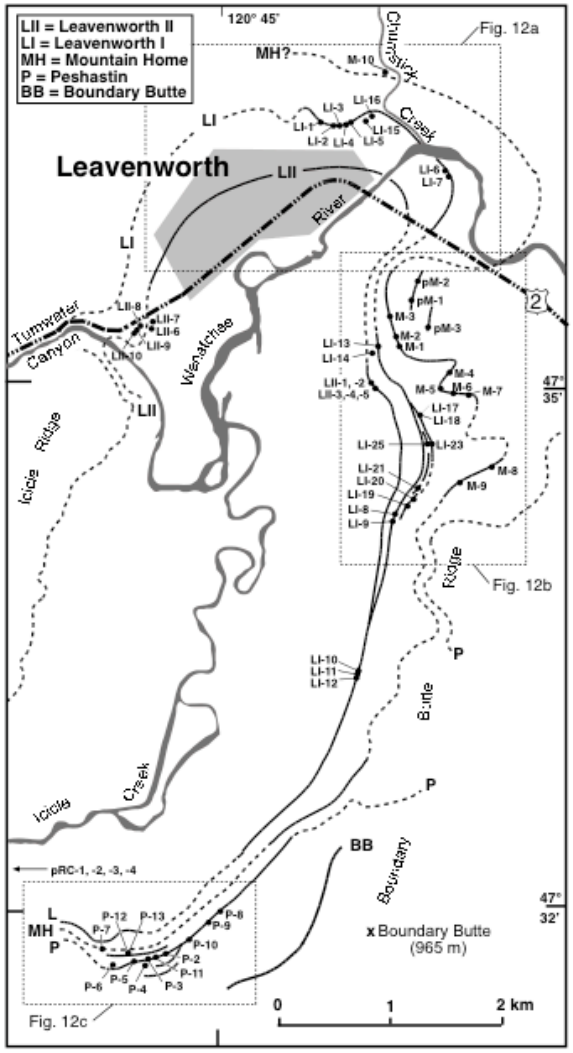

Porter & Swanson, Figure 10

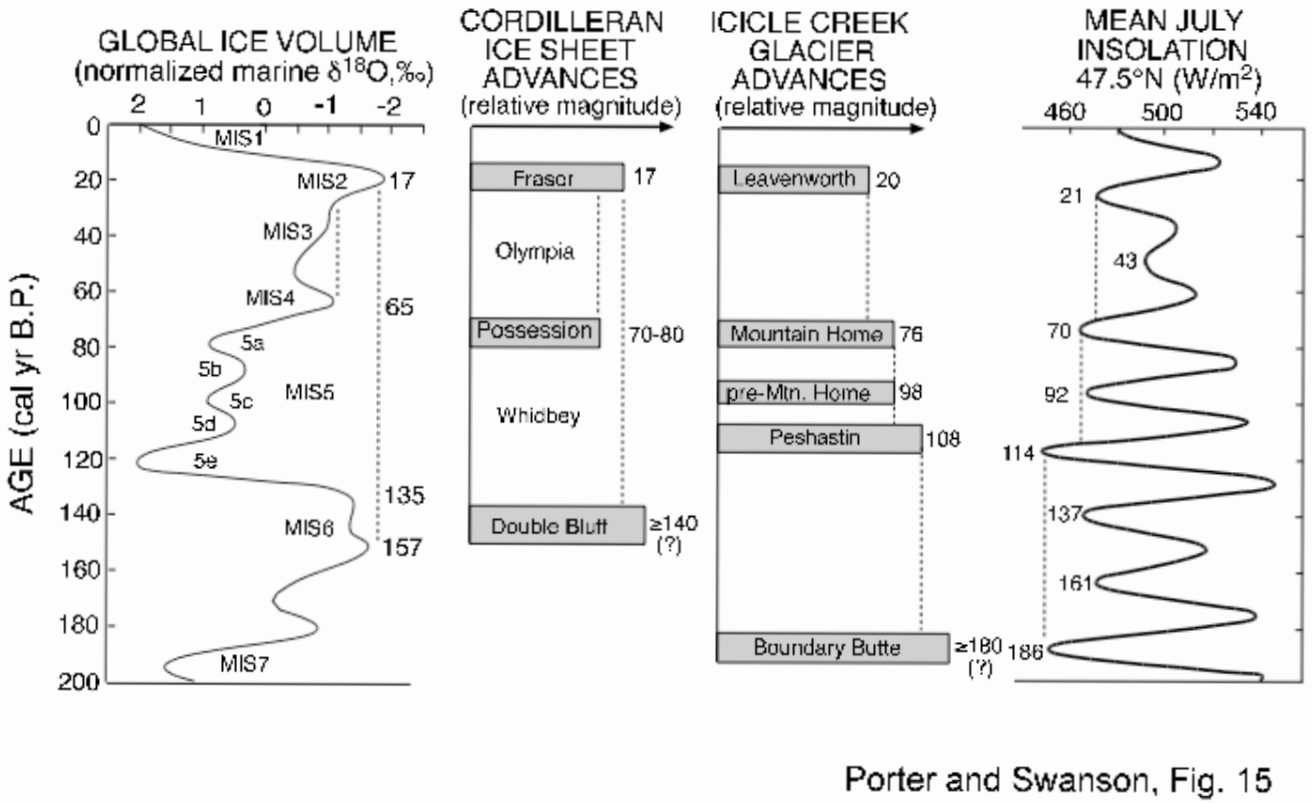

Porter and Swanson, Fig. 15

The timing of glacial advance in the Icicle Creek drainage is correlative with periods of major ice volume as documented by the MIS record, but the magnitude of each respective advance is more consistent with the Mean July Insolation record.

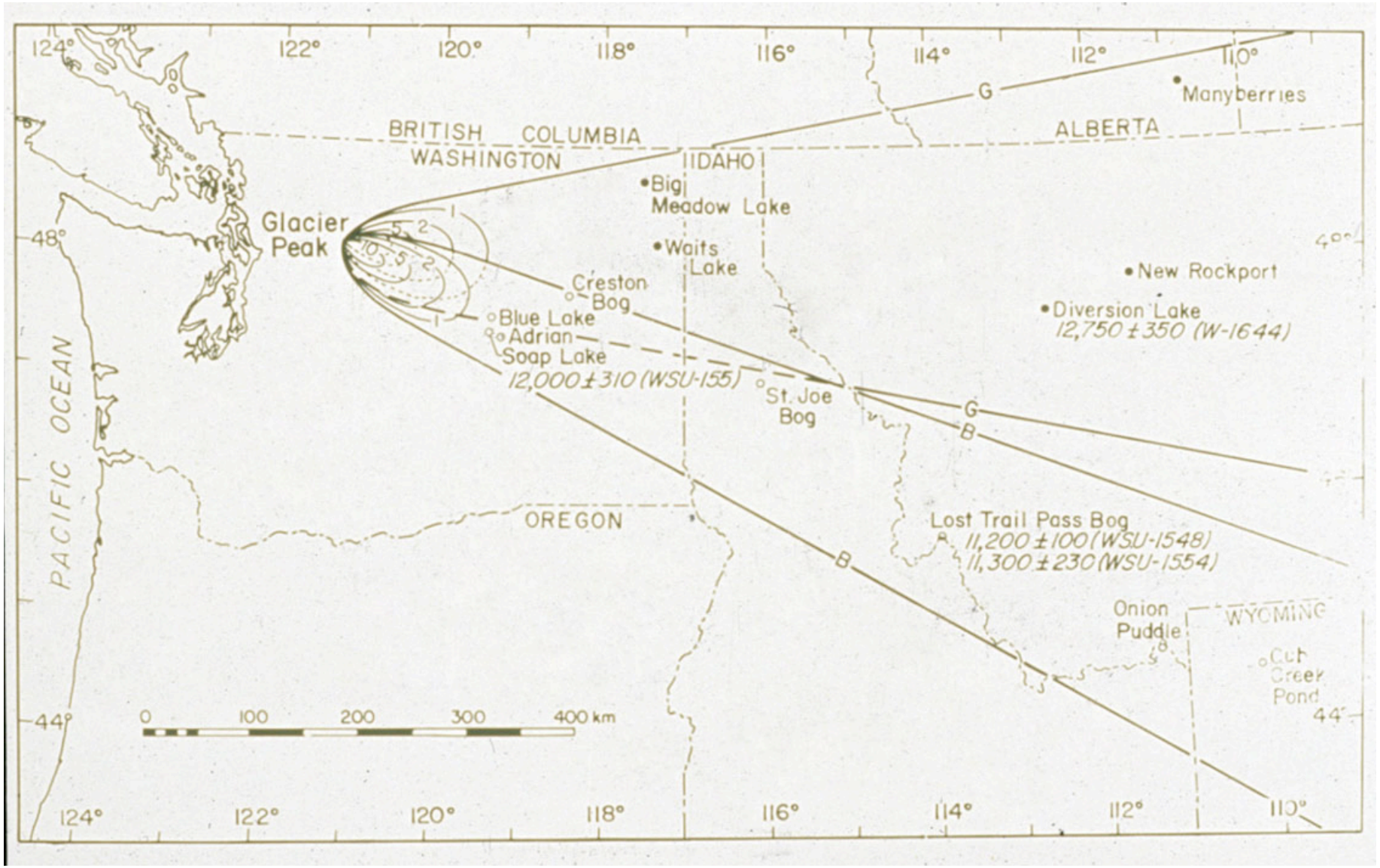
124°
122°
120°
118°
116°
114°
112°
110°
48°
44°
40°
G
B
Manyberries
BRITISH COLUMBIA
WASHINGTON
IDAHO
ALBERTA
Big Meadow Lake
Glacier Peak
Waits Lake
New Rockport
Creston Bog
Diversion Lake
12,750 ± 350 (W-1644)
Blue Lake
Adrian
Soap Lake
12,000 ± 310 (WSU-155)
St. Joe Bog
PACIFIC OCEAN
OREGON
Lost Trail Pass Bog
11,200 ± 100 (WSU-1548)
11,300 ± 230 (WSU-1554)
Onion Puddle
WYOMING
Cub Creek Pond
0 100 200 300 400 km